Immediate Deflections of Simply Supported, Bonded, Class T and Class C Prestressed Concrete Beams

by

Hayden Yendle Hughes

A thesis submitted to the Graduate Faculty of
Auburn University
in partial fulfillment of the
requirements for the Degree of
Master of Science

Auburn, Alabama
May 5, 2023

Keywords: effective moment of inertia, flexure, modulus of elasticity, partial prestressing, serviceability, slabs, structural design

Approved by

Robert W. Barnes, Ph.D., P.E., Chair, Brasfield & Gorrie Associate Professor of Civil Engineering
Anton K. Schindler, Ph.D., P.E., Mountain Spirit Professor of Civil Engineering
Justin D. Marshall, Ph.D., P.E., Associate Professor of Civil Engineering

ABSTRACT

Design practice for prestressed members has moved toward allowing partially prestressed members, which are allowed to crack under service loads. To define design requirements, the ACI 318 Building Code explicitly defines different classes of prestressed flexural members. A simple procedure for computing immediate service-load deflections that accurately incorporates the effects of cracking in Class T and Class C partially prestressed concrete members is not yet standardized.

The primary focus of this study is to propose and evaluate the accuracy of a simple method for estimating the immediate deflections of cracked prestressed flexural members subjected to service loads. To achieve this a database of tests representing only beams expected to crack under service loads was created from published data and used to compare four methods of calculation of deflection. The outputs of the methods were compared to reported measured deflection values at key service-load stress levels. Conclusions were made about which of the methods provided accurate results. The methods differed in approach when calculating the effective moment of inertia, cracked moment of inertia, and identifying the load level at which the transition of uncracked behavior transitions into cracked behavior.

Overall, of the four methods compared, the proposed method was found to be the most accurate method when predicting immediate deflections for cracked, prestressed flexural members. The proposed method uses a cracked-section moment of inertia calculated including prestressing effects, a decompression moment at which uncracked behavior transitions to cracked behavior, and an effective moment of inertia based on moment ratios relative to the decompression moment.

ACKNOWLEDGMENTS

To my Lord, thank you for the perseverance you have blessed me with and support system you gave me to reach this accomplishment.

To my husband Heath and daughter Millie, thank you for your patience and support through the long hours after work or on the weekends where I was not able to be as available as I would have liked to have been. To my parents Simon and Karen, there is not enough thanks for all the support, prayers, and encouragement you have given me throughout my entire life and this college experience. I am who I am and where I am because you push me to be the best. I hope to continue making you proud in all I do. To my in-laws Brian and Pam, thank you for the extra babysitting and prayers through this phase of my life. It means so much that you would take your time to watch my baby so that I can reach a goal of mine. I want to thank the rest of my family, Meghan, Lauren, Hannah, Helen, Donnie, Joanne, and Alan for praying for me and encouraging me through this process as well. Love you all.

I am extremely honored to have Dr. Barnes as my advisor, role model, and friend through this process. I hope my work reflects well on him as I could not have done this without his patience, flexibility in his time, and amazing knowledge. To my LBYD work family, thank you for the support, understanding, and flexibility of work hours to be able to achieve this accomplishment. Paige Cummings, thank you for the help you provided me with pulling and rechecking my data for all the specimens as I know it was tedious and time-consuming work.

I have been overwhelmed by amount of love and support through this whole process and cannot express how much thanks I owe everyone in through this process. Looking forward to moving onto the next chapter of life that God has prepared for me and my family!

TABLE OF CONTENTS

ABSTRACT 2

ACKNOWLEDGMENTS 3

TABLE OF CONTENTS 4

LIST OF FIGURES 6

LIST OF TABLES 7

CHAPTER 1: INTRODUCTION 8

1.1 BACKGROUND 8

1.2 RESEARCH OBJECTIVES AND SCOPE 8

1.3 ORGANIZATION OF THESIS 9

CHAPTER 2: METHODS FOR COMPUTING IMMEDIATE DEFLECTIONS OF CRACKED PRESTRESSED CONCRETE BEAMS 10

2.1 INTRODUCTION 10

2.2 COMPUTING IMMEDIATE DEFLECTIONS OF CRACKED NONPRESTRESSED REINFORCED CONCRETE BEAMS 10

2.3 METHODS FOR COMPUTING IMMEDIATE DEFLECTIONS OF CRACKED PRESTRESSED CONCRETE BEAMS 12

2.3.1 Translating I_E Method To Prestressed Concrete 13

2.3.2 What I_{cr} to Use in I_E? 18

2.3.3 Bischoff's Rational and Trilinear Methods 19

2.3.4 Design Example 22

CHAPTER 3: DATABASE OF CLASS T AND CLASS C FLEXURAL TEST RESULTS 23

3.1 INTRODUCTION 23

3.2 BEAM RESEARCH STUDIES 23

3.2.1 Criteria Used in Selecting Beams to be Used in this Study 26

3.2.2 Database Data Provided 27

3.2.3 Key Service Load Levels 30

CHAPTER 4: EVALUATING THE ACCURACY OF PREDICTION METHODS 32

4.1 INTRODUCTION 32

4.2 RESULTS 33

4.3 DISCUSSION 45

CHAPTER 5: RESEARCH CONCLUSIONS AND RECOMMENDATIONS 53

5.1 SUMMARY OF WORK 53

5.2 CONCLUSIONS 53

5.3 RECOMMENDATIONS FOR FUTURE RESEARCH 54

REFERENCES 55

APPENDIX A: NOTATION 58

APPENDIX B: CALCULATION EXAMPLES 62

APPENDIX C: DATABASE OF CLASS T AND CLASS C SIMPLY SUPPORTED PRESTRESSED BEAM TESTS 79

LIST OF FIGURES

Figure 2-1: Normalized moment-deflection curve for a nonprestressed reinforced concrete flexural member (adapted from Branson [1977]) 11

Figure 2-2: I_e concept for service load deflection computations in cracked prestressed members (adapted from Branson [1977]) 14

Figure 2-3: Proposed I_e procedure—use of decompression moment as transition point for I_e..... 16

Figure 2-4: Simplified Trilinear Method approach for computing deflection (Bischoff Naito Ingaglio 2018) 21

Figure 4-1: Comparison of prediction methods at a tension stress level of 10f'c. 45

Figure 4-2: Comparison of prediction methods at a tension stress level of 12f'c. 46

Figure 4-3: Comparison of prediction methods at the maximum reasonable service-level load.. 46

Figure 4-4: Comparison of prediction methods used for Class T members at the maximum reasonable service-level load. 47

Figure 4-5: Comparison of prediction methods used for Class C members at the maximum reasonable service-level load. 47

Figure 4-6: Distribution of prediction accuracy at key service load levels 48

Figure 4-7: Distribution of prediction accuracy for Class T beams, Class C beams, and all beams at the maximum reasonable service load 50

Figure 4-8: Histogram of prediction accuracy by member class at 7.5f'c stress level. 51

Figure 4-9: Histogram of prediction accuracy for all tests at 7.5f'c stress level. 52

Figure 4-10: Distribution of prediction accuracy for Class T beams, Class C beams, and all beams at 7.5f'c stress level.. 52

Figure A-1: 10DT24 from PCI Design Handbook 62

LIST OF TABLES

Table 4-1: Measured and predicted deflections in Class T beams at 7.5f'c tension stress level .. 34

Table 4-2: Measured and predicted deflections in Class T beams at 10f'c tension stress level ... 35

Table 4-3: Measured and predicted deflections in Class T beams at maximum tension stress level 36

Table 4-4: Measured and predicted deflections in Class C beams at 7.5f'c tension stress level .. 37

Table 4-5: Measured and predicted deflections in Class C beams at 10f'c tension stress level ... 39

Table 4-6: Measured and predicted deflections in Class C beams at 12f'c tension stress level ... 41

Table 4-7: Measured and predicted deflections in Class C beams at maximum tension stress level 43

Table C-1: Specimen Identification, Cross-Sectional Properties, and Concrete Material Properties 79

Table C-2: Specimen Reinforcement Properties 83

Table C-3: Specimen Span and Loading Geometry, Midspan Bending Moments, and ACI 318 Prestressing Classification 87

Table C-4: Midspan Deflections (from original sources) for Specific Levels of Midspan Bending Moment 91

CHAPTER 1: INTRODUCTION

1.1 BACKGROUND

Prestressed members were historically designed to remain uncracked under service loads (i.e., “fully prestressed”). When that was standard practice, calculating immediate deflections under service loads was straightforward and based on uncracked section properties. In the late 20th century, design practice started to move toward allowing partially prestressed members, which were allowed to crack somewhat under service loads. This then presented the problem of how to compute the deflections due to service loads for cracked prestressed concrete members. Beginning with the 2002 ACI Building Code Requirements for Structural Concrete (ACI Committee 318 2002), different classes of prestressed flexural members were explicitly defined, and classification now corresponds to the level of tensile stress in the extreme fiber of the section under service load assuming an uncracked section. Class T and Class C members are allowed to crack under service loads. Cracking was to be accounted for in the design checks for these members, but a simple procedure for computing immediate service-load deflections that accurately incorporates the effects of cracking in these partially prestressed concrete members has not yet gained consensus endorsement for ACI 318 adoption.

1.2 RESEARCH OBJECTIVES AND SCOPE

The primary objective of this thesis is to propose and evaluate the accuracy of a simple, clear method for estimating the immediate deflections of Class T and Class C prestressed flexural members subjected to service loads. To achieve this objective a database of tests that are representative of beams designed to crack under service loads was established and used to compare different methods of deflection calculation.

The database was created by compiling multiple tests from papers that mostly predate the creation of ACI 318 Class T and Class C member classifications. The beam tests were filtered to obtain a set of tests of only beams that could realistically be considered Class T or C prestressed flexural members according to current ACI 318 (2019) requirements. Once the database was compiled, the accuracy of four methods of calculating deflection was evaluated by comparing predicted service-load deflections to the deflections reported by the original researchers.

1.3 ORGANIZATION OF THESIS

Chapter 2 outlines the historical background of simplified methods for estimating immediate service-load deflections for structural concrete permitted to crack under service loads. The chapter begins with an overview of a long-standing method for cracked, nonprestressed concrete then describes issues related to the extension of this approach to cracked prestressed concrete members. The author's proposed approach to the problem is described. The chapter also describes two other proposed approaches to calculating immediate deflection for prestressed concrete members.

Chapter 3 describes the database compiled to assess the accuracy of methods proposed for computing immediate service-load deflections of Class T and Class C flexural members. The descriptions include the process and criteria used to select tests so as to focus on specimens that could realistically be considered Class T or Class C because most tests were performed before these classes were defined.

Chapter 4 shows results and comparisons of the four methods looked at in predicting immediate deflections. Inaccuracies of the outputs of each method are discussed.

Chapter 5 provides a summary and conclusions of the research. Recommendations for future research are provided.

CHAPTER 2: METHODS FOR COMPUTING IMMEDIATE DEFLECTIONS OF CRACKED PRESTRESSED CONCRETE BEAMS

2.1 INTRODUCTION

This chapter provides historical background for simplified methods for estimating immediate deflections under service loads for structural concrete flexural members permitted to crack under service loads. It begins with an overview related to a common, long-standing method of calculation of immediate service-load deflections of cracked nonprestressed reinforced members. After outlining some of the potential complications of extending this method to cracked prestressed concrete members, it describes a proposed procedure for doing so. Two other recently proposed approaches are also described herein.

2.2 COMPUTING IMMEDIATE DEFLECTIONS OF CRACKED NONPRESTRESSED REINFORCED CONCRETE BEAMS

The calculation of immediate service-load deflections of nonprestressed reinforced concrete flexural members for checking against permissible limits in ACI 318 has long been based on using general elastic deflection formulas. This is accomplished with sufficient accuracy by combining the elastic concrete modulus of elasticity, E_c, with an "effective" moment of inertia, I_e, that simultaneously accounts for (a) the nonlinear effects of tension stiffening after the member begins to crack, and (b) the extent of the cracking zone along the span of the member. Branson (1963) developed an expression for I_e that used boundaries where I_e falls between (a) the moment of inertia of the uncracked cross section and (b) the moment of inertia of the cracked, linear-elastic cross section, I_{cr}, as seen in Figure 2-1.

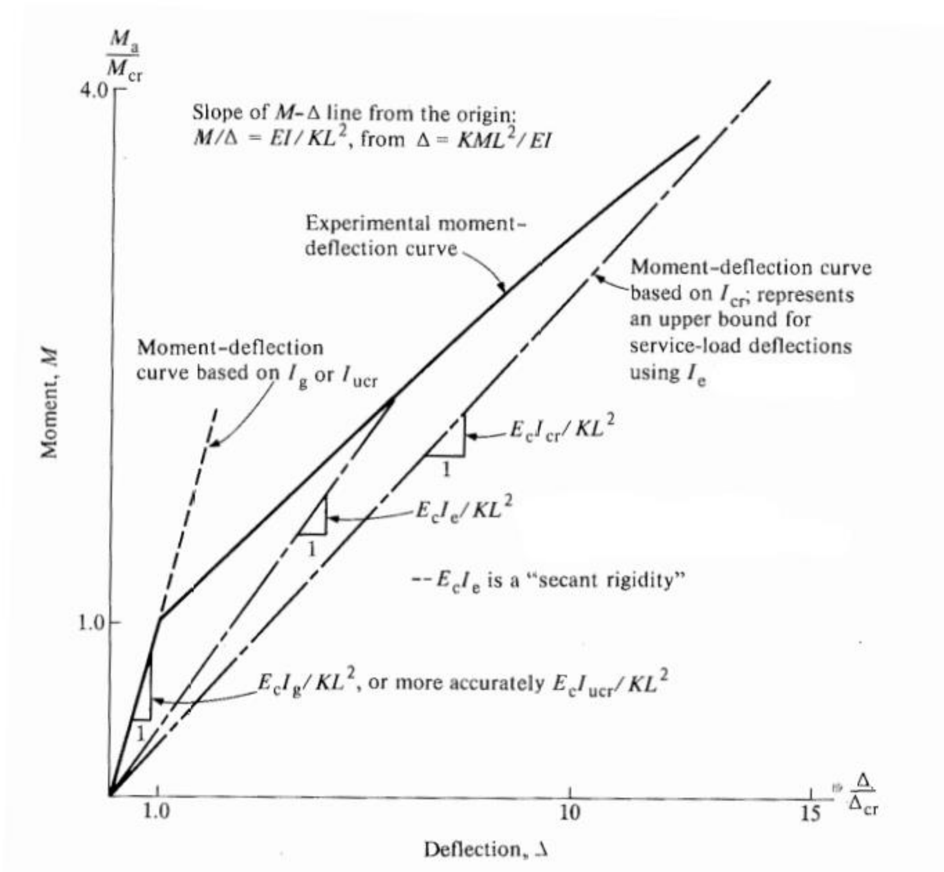

Figure 2-1: Normalized moment-deflection curve for a nonprestressed reinforced concrete flexural member (adapted from Branson [1977])

The relative value of I_e between these bounds was determined by Branson (1963) to depend on the magnitude of the bending moment at the critical cross section, M_a, relative to the moment expected to cause cracking, M_{cr}, at the same section. After research conducted at Auburn University, Branson concluded that this moment ratio (M_{cr}/M_a) should be raised to a power of 4 when determining the effective moment of inertia near an individual cracked cross section, but that a power of 3 was more appropriate when determining an average effective moment of inertia for use over the entire length of a simple reinforced concrete beam, resulting in Equation 2-1.

$$I_e = \left(\left(\frac{M_{cr}}{M_a}\right)^3\right) I_g + \left[1 - \left(\left(\frac{M_{cr}}{M_a}\right)^3\right)\right] I_{cr} \qquad \textit{Equation 2-1}$$

Here I_e is computed as a weighted average of the uncracked section and cracked section moments of inertia (I_g and I_{cr}, respectively), with the moment ratio raised to the third power as the weighting factor. Branson (1963) deemed the use of the gross moment of inertia (I_g) for the uncracked section to be an adequate simplification. This effective moment of inertia formula was adopted in ACI 318 soon thereafter and remained in use until modified in 2019 (ACI 318 2019). To determine the immediate deflection of a cracked, simply-supported, nonprestressed concrete beam or one-way slab, this value of I_e is simply combined with E_c to form the rigidity (EI) in the appropriate linear-elastic deflection formula for the applied loading under consideration.

2.3 METHODS FOR COMPUTING IMMEDIATE DEFLECTIONS OF CRACKED PRESTRESSED CONCRETE BEAMS

If prestressed beams are not cracked under service loads (i.e., they are "fully prestressed"), calculating the immediate deflection of prestressed beams is a simple, straightforward process using the uncracked section properties (or gross section properties for simplicity). In 2005, ACI 318-05 formally introduced new classifications for prestressed flexural members—defining Class T and Class C prestressed flexural members, which would be expected to crack under service loads, based on computed extreme-fiber tension stresses (often referred to as "partially prestressed" members).

ACI 318-19 R24.5.2.1 currently defines three classes of behavior of prestressed flexural members based on computed extreme-fiber tension stresses under service loads. Class U members are members that have a computed service-load tension stress that does not exceed $7.5\sqrt{f'_c}$ and are thus assumed to behave as uncracked under service loads (often referred to as "fully prestressed" members). Class T members are defined as having a calculated service-load tension stress falling between $7.5\sqrt{f'_c}$ and $12\sqrt{f'_c}$. Class C members are defined as having a calculated service-load tension stress greater than $12\sqrt{f'_c}$. Thus, Class T and Class C represent increasing levels of "partially prestressed" behavior, with nonprestressed concrete falling at the far end of the spectrum.

These newly defined classes of partially prestressed members intensified a need to be able to calculate immediate service-load deflections for cracked prestressed members for checking against allowable deflection limits. When viewed within the framework of an effective moment of inertia method of computing deflections, several issues arise and warrant discussion prior to application.

2.3.1 Translating I_E Method To Prestressed Concrete

One issue that must be addressed when applying Branson's I_e method to prestressed concrete members is the level of bending moment at which to initiate application of this I_e. ACI 318 (2019) Section 24.2.3.9 has retained the use of the Branson (1963) I_e for use with cracked (Class T and Class C) prestressed members but has not yet explicitly addressed this question. The Commentary (R24.2.3.9) cites a variety of sources with potential alternative methods, but ACI 318 itself implies the use of I_e over the full range of applied loading. An issue with this approach is that the Branson I_e is based on nonprestressed behavior in which the tension face of the beam goes into tension as soon as a load is applied and cracking initiates under relatively small service loads. However, a prestressed beam has a precompression force and moment that keep the tension face in compression until a much higher bending moment is applied to the beam.

Shaikh and Branson (1970) addressed this issue by proposing a modification where the beam is treated as uncracked for deflections up to the dead load moment and the Branson (1963)

I_e is only computed for and applied to the portion of loading beyond the dead load. This technique is also adopted in the PCI Design Handbook (up to the current 8th edition). Figure 2-2 adapted from Branson (1977) shows a typical moment versus deflection curve of a prestressed beam. The smaller axis origin located at the dead load moment in Figure 2-2 represents the starting point where an effective moment of inertia corresponding to nonprestressed beam behavior would start.

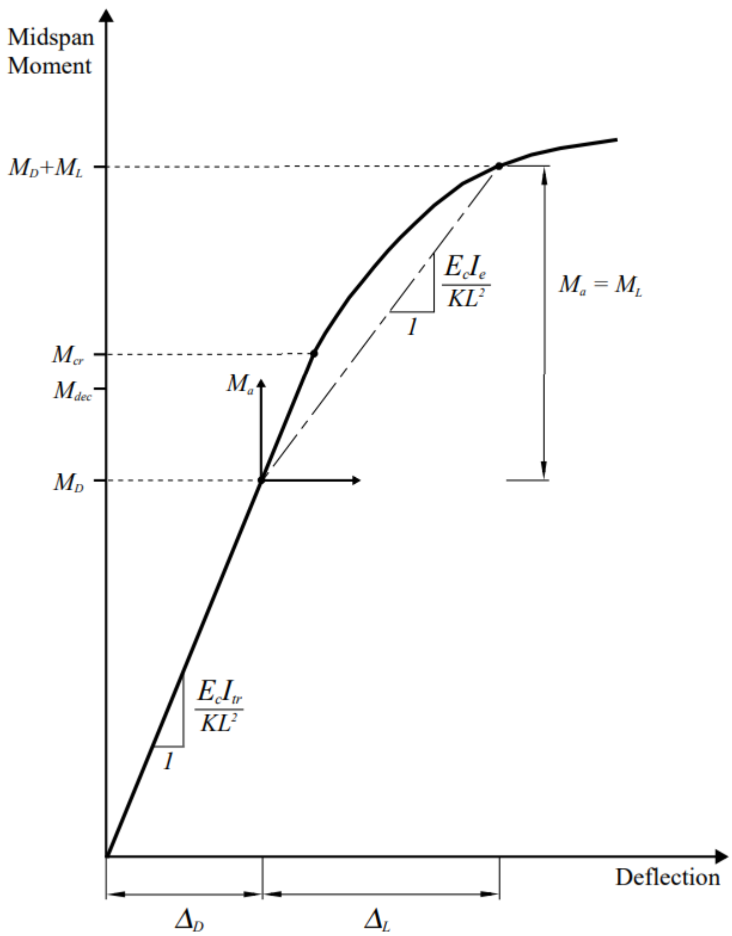

Figure 2-2: I_e concept for service load deflection computations in cracked prestressed members (adapted from Branson [1977])

A related issue is the moment ratio (M_{cr}/M_a) to be used to reflect the extent of cracking in the I_e formulation. In the original formulation for nonprestressed concrete, both M_{cr} and M_a are implicitly measured from a state of zero stress on the cross section. However, for prestressed concrete, a significant portion of the applied bending moment (and the resisting cracking moment, M_{cr}) are exhausted before the precompression of the cross section is overcome. Therefore, a specific value of M_{cr}/M_a represents a different extent of cracking in a nonprestressed beam than in a prestressed beam. The method proposed by Shaikh and Branson (1970) employs the ratio of the *portions* of M_{cr} and applied moment that exceed the dead load moment (M_D). This approach is implicitly adopted in the PCI Design Handbook (PCI 2017) I_e formulation.

The more theoretically correct approach of using the decompression moment, M_{dec}, (moment at which the bottom fiber overcomes the precompression stress) as the transition moment from prestressed to nonprestressed behavior, is depicted in Figure 2-3. This method of using M_{dec} as the transition moment is the closest to representing the fundamental flexural behavior of a prestressed concrete beam as the superposition of a nonprestressed concrete beam (with an effective moment of inertia, I_e) onto a precompression moment equal to $M_{dec.}$ Because the precompressed portion of the cross section first experiences tension when the applied bending moment equals M_{dec}, this is the logical level of moment to use as the basis for correspondence with nonprestressed behavior (as represented by I_e).

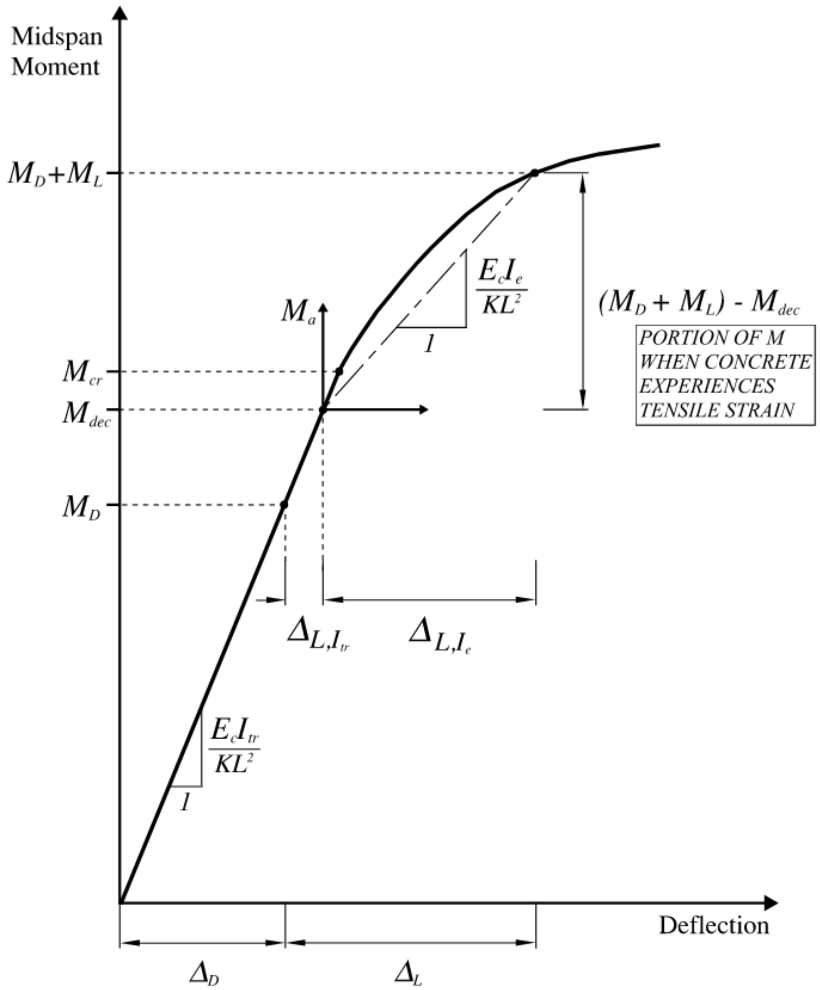

Figure 2-3: Proposed I_e procedure—use of decompression moment as transition point for I_e

While the Shaikh and Branson (1970) method of using the dead-load moment as the transition moment does make for simpler, single-increment live-load deflection calculations, the more fundamentally sound approach of using M_{dec} as the transition moment should be more accurate over a wider range of partially prestressed members. There is no reliable relationship between the dead load moment and the decompression moment. In fact, the disparity between the dead load moment and M_{dec} is likely to be considerably different for Class C members than for Class T or Class U (uncracked) members. Furthermore, the accuracy associated with using the dead-load moment as the transition moment can be expected to vary for the same prestressed member when used in two different design scenarios with different proportions of dead and live load.

Therefore, the I_e method proposed in this thesis for Class T and Class C prestressed flexural members employs two modifications based on the establishment of the decompression moment (M_{dec}) as the transitional moment from fully prestressed behavior to cracked behavior:

1) The effective moment of inertia (I_e) should only be used for the *portion* of the applied moment exceeding M_{dec} at the critical section for cracking. The moment of inertia of the uncracked section (or I_g for simplicity) should be used for the portion of the applied moment up to M_{dec}.
2) The moment ratio used in computing I_e should be based on the portions of (applied and resisting) moments beyond M_{dec}. (i.e., the moment portions corresponding to tension in the concrete):

$$I_e = \left[\left(\frac{M_{cr} - M_{dec}}{M_a - M_{dec}}\right)^3\right] I_g + \left[1 - \left(\frac{M_{cr} - M_{dec}}{M_a - M_{dec}}\right)^3\right] I_{cr} \qquad \textit{Equation 2-2}$$

In general, these proposed modifications are not new; Naaman (1985) and ACI Committee 423 (ACI 423.5R 1999) both reported "general agreement" among researchers on this modified approach but noted some ongoing disagreement about specific definitions of M_{dec} and I_{cr} for prestressed members. For example, Chen (1973) proposed a different definition for the decompression moment. In the method proposed in this thesis, M_{dec} is defined as the moment that corresponds to zero stress at the location where cracking is first expected (e.g., the bottom fiber under positive bending moment). This definition of decompression moment (M_{dec}) is common (e.g., Bachmann 1984).

2.3.2 What I_{cr} to Use in I_E?

As noted above, there has been substantial difference of opinion on how I_{cr} should be defined or calculated to represent the cracked-section moment of inertia for prestressed concrete members for use in the I_e equation. Shaikh and Branson (1970) used what is often referred to as the "fully cracked" moment of inertia, which neglects the influence of the prestressing force on the flexural rigidity of the cracked cross section (i.e., computed as if the prestressed reinforcement was not prestressed). This is a very simple and conservative approach, but it does not accurately account for the effect of prestressing force on the neutral axis position and curvature in a cracked prestressed beam (Nilson 1976; Moustafa 1977; Boczkaj 1994; Mast 1998; Bischoff, Naito, and Ingaglio 2018). A more accurate approach would be to use I_{cr} that accounts for the precompression in the beam; however, this "partially cracked" I_{cr} varies with the bending moment applied to the cross section. Branson (1983) noted that he employed the "fully cracked" I_{cr} because it required much less calculation to reach an approximate value. Mast (1998) has since expanded on a practical method to determine accurate cracked-section properties, stresses, and curvature including the effects of the prestressing force through the use of simple computing applications to handle the iterative calculations often required. With the advancement of technology, this I_{cr} can be easily computed using a spreadsheet and solver routine.

The method proposed in this thesis employs the cracked-section I_{cr} value that includes the effect of the prestress force and is evaluated at a bending moment equal to the total service-load moment under consideration—in other words, the "partially cracked" value or Mast (1998) approach. This is the value of I_{cr} that should be used in the Proposed Method for I_e given in Equation 2-2. Using this I_{cr} is more accurate theoretically than using a ("fully cracked") value that neglects the prestress force, and it is still slightly conservative because it is (a) evaluated at the peak value of applied bending moment, and (b) less than the secant cracked-section I_{cr} on which the original Branson I_e equation is based. The computation of I_{cr} should also include the influence of any nonprestressed reinforcement in the member. Because Class T and (especially) Class C prestressed members often rely on nonprestressed tension reinforcement to provide a portion of their flexural strength, the inclusion of the stiffness added by this reinforcement is important for accurate estimation of service-load deflections when cracked.

In order to see the effect of implementing the simpler, "fully cracked" I_{cr} that neglects the prestress force (used by Shaikh and Branson [1970]), predictions computed by substituting the "fully cracked" I_{cr} from Equation 2-2 into the Proposed Method were performed. These predictions are referred to as the "Branson No P" Method in Chapter 4 of this thesis.

2.3.3 Bischoff's Rational and Trilinear Methods

Bischoff (2005, 2007) introduced another method of calculating I_e. This approximation for nonprestressed members was in response to Branson's method not being very accurate when beams had atypical amounts of steel. This method was adapted further by Bischoff, Naito, and Ingaglio (2018) as the "Rational" method for prestressed concrete beams, in which an offset or "shift" moment, M_1, is where the change in moment of inertia occurs, as seen in Equation 2-3 (Bischoff, Naito, and Ingaglio 2018). This shift moment is typically greater than the decompression moment used in the method proposed in this thesis.

$$I_e^* = \frac{I_{cr}}{1 - (\frac{M_{cr} - M_1}{M_a - M_1})^2 (1 - {I_{cr}}/{I_g})} \qquad \textit{Equation 2-3}$$

$$M_1 = \frac{\left[M_0 - M_{zc}\left(\frac{I_{cr}}{I_g}\right)\right]}{(1 - \frac{I_{cr}}{I_g})} \qquad \textit{Equation 2-4}$$

Equation 2-3 is only valid if the applied moment, M_a, is greater than the cracking moment, M_{cr}, ($M_a > M_{cr}$) *and* the shift moment, M_1, using Equation 2-4 (Bischoff, Naito, and Ingaglio 2018), is less than M_{cr} ($M_1 < M_{cr}$). Equation 2-3 and Equation 2-4 use a "fully cracked" value of I_{cr} (i.e., neglecting the influence of the prestress force on the moment of inertia).

When the shift moment is greater than the cracking moment ($M_1 > M_{cr}$), then Equation 2-5 (Bischoff, Naito, and Ingaglio 2018) is applied, in which the new shift moment, M'_1, from Equation 2-6 (Bischoff, Naito, and Ingaglio 2018) uses the "partially cracked" value of I'_{cr} to reach a better evaluation of an effective moment of inertia, I^*_e, (i.e., the second possible value) if M'_1 does not exceed M_{cr}. However, if the new shift moment, M'_1, is greater than M_{cr}, then the prescribed value of I^*_e (i.e., the third possible value) is the unmodified value of the "partially cracked" I'_{cr}.

$$I_e^* = \frac{I'_{cr}}{1 - (\frac{M_{cr} - M'_1}{M_a - M'_1})^2 (1 - {I'_{cr}}/{I_g})} \qquad \textit{Equation 2-5}$$

$$M'_1 = \frac{\left[M'_0 - M_{zc}\left(\frac{I'_{cr}}{I_g}\right)\right]}{(1 - \frac{I'_{cr}}{I_g})} \qquad \textit{Equation 2-6}$$

The Trilinear Method proposed by Bischoff, Naito, and Ingaglio (2018) simplifies the Rational Method by decreasing the amount of conditional checks used. An intermediate moment of inertia, which is denoted as I''_{cr} and calculated using Equation 2-7 (Bischoff, Naito, and Ingaglio 2018), transitions from the gross-section moment of inertia, I_g, to the "fully cracked" I_{cr} as shown in Figure 2-4. This method also simplifies the Rational Method by not requiring an iterative approach to reach a "partially cracked" I'_{cr} and other properties of a "partially cracked" section.

$$I"_{cr} = \left[\frac{(M" - M_{cr})}{(M" - M_0) - (M_{cr} - M_{zc})\left(\frac{I_{cr}}{I_g}\right)}\right] I_{cr} \qquad \textit{Equation 2-7}$$

This calculation uses boundaries of a shift moment, *M"*, which is the greater value of (a) 1.5 multiplied by the (zero-curvature) prestress moment, M_0, or (b) the moment corresponding to the upper limit of Class T. This method may have up to three branches of deflection to be calculated: the uncracked properties up to cracking, an "intermediate" cracking moment of inertia I''_{cr} as calculated in Equation 2-7, and then if the applied moment exceeds the intermediate boundary *M"* (M_a > *M"*) then the "fully cracked" I_{cr} is applied.

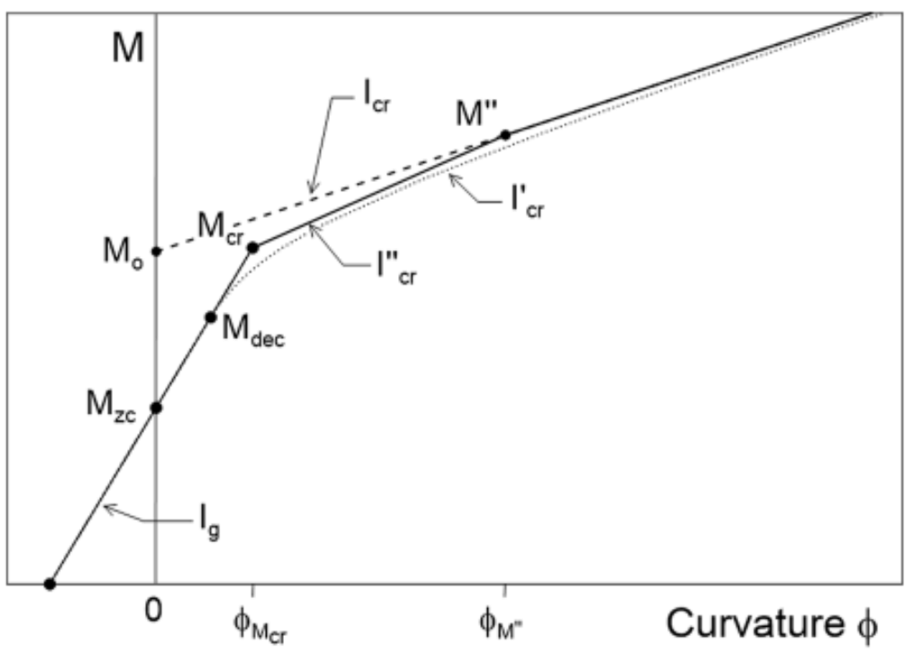

Figure 2-4: Simplified Trilinear Method approach for computing deflection (Bischoff, Naito, and Ingaglio 2018)

2.3.4 Design Example

In order to better explain and illustrate the method proposed in this chapter, as well as the other methods discussed, application of all four methods to a standard example beam from the PCI Design Handbook (2017) is presented in Appendix B. Detailed, annotated calculations are included.

CHAPTER 3: DATABASE OF CLASS T AND CLASS C FLEXURAL TEST RESULTS

3.1 INTRODUCTION

This chapter describes the flexural test results collected for the database along with the criteria used to select the test specimens that represent members that represent Class T and Class C prestressed members. The chapter then continues to describe the database configuration and the importance of the entries chosen to be presented in the database itself which can be found in Appendix C of this thesis.

3.2 BEAM RESEARCH STUDIES

This database comprises 106 beam flexural tests from nine research studies ranging from 1956 to 2015.

Janney et al. (1956) test specimens consist of rectangular cross sections with an overall depth of 12 inches and clear span of 9 feet each loaded with a single midspan load. Each test specimen contained different amounts of prestressing reinforcement and was either pre- or post-tensioned. Some specimens in this study had unbonded prestressing or had nonprestressed reinforcement. Bonded prestressing had slightly rusted reinforcement to achieve a better bond. The tests predate low-relaxation strands and have relatively high loss of prestress. After applying the selection criteria to the tests in this study, six tests were included in the database.

Sozen (1957) reported tests of rectangular or I-shaped cross sections with an overall depth of 12 inches and clear spans ranging from 7 to 9 feet. Tests were loaded either with a single midpoint load or two symmetrically placed point loads. Each test contained different amounts of prestressing reinforcement and was either pre- or post-tensioned. Some tests in the study had little to no prestressing and/or concrete strength less than 3,000 psi. The focus of this study was to look at the shear strength so the limiting load for each test might be controlled by when a shear crack opens. After applying the selection criteria to all tests in this study, 33 tests were included in the database.

Hernandez (1958) reported I-shaped test specimens with an overall depth of 12 inches and clear span of 9 feet. Tests included either a single midpoint load or two symmetric point loads. Each test contained different amounts of prestressing reinforcement; all specimens were pretensioned. This study was a continuation of the Sozen (1957) study and has similarities in the focus on shear as well as little to no prestressing in some tests and low concrete strengths. After applying the selection criteria, 20 tests were included in the database.

Warwaruk (1960) reported tests of rectangular beams with an overall depth of 12 inches and a clear span of 9 feet each loaded with two symmetric point loads. Each test contained different amounts of prestressing reinforcement and were either pre- or post-tensioned. There are some tests in this overall study that had partially bonded or intentionally unbonded reinforcement to replicate potential construction flaws. These were discarded from further consideration. After applying the selection criteria, 20 tests were included in the database.

Shaikh (1967) reported 12 tests of rectangular beams with an overall depth of 8 inches and clear span of 15 feet each loaded with two symmetric point loads. Each test contained different amounts of prestressing reinforcement and was pretensioned. Some tests in this study contain nonprestressed reinforcement. The nonprestressed reinforcement used was either prestressing steel referred to as “Non-tensioned High Strength Steel”, 33 ksi minimum yield strength steel, or 60 ksi minimum yield strength steel. Another characteristic noted about this study is that the change in concrete strains were measured between the time that the strands were prestressed to the time of the test instead of reporting a stress in the reinforcement at the time of the test. After applying the selection criteria, all 12 tests were included in the database.

Aswad et al. (2004) reported three full-scale, pretensioned double-tee tests with an overall depth of 30 inches and clear span of 62 feet. A uniform load was approximated for each test using concrete blocks. Each test contained different amounts of prestressing reinforcement. All three tests satisfied the selection criteria and were included in the database.

Saqan and Frosch (2009) reported tests of pretensioned, rectangular beams with an overall depth of 28 inches and clear span of 13.33 feet each loaded with a single midpoint load. Each specimen contained different amounts of prestressing reinforcement. The focus of this study was to look at the shear strength, so the limiting load for each test might be controlled by when a shear crack opens. A notable feature of this study is that it included three series of test specimens all with approximately the same total effective prestress force. This effective prestress force was achieved in each series with a different combination of prestressed reinforcement area and effective prestress level. The amount of nonprestressed reinforcement varied for each specimen in a series. After applying the selection criteria, eight tests were included in the database.

Brewe and Myers (2011) reported T-beam tests with an overall specimen depth of 12 inches and a clear span of 14.5 feet; each loaded with two symmetric point loads. Each test contained different amounts of pretensioned reinforcement. Some tests in this study were designed to fail in shear under non-symmetric loading. After applying the selection criteria, three tests were included in the database.

Naito et al. (2015) reported a study that evaluated many different types of testing for quality assurance. The beams that underwent flexure testing had rectangular cross-sections, a 6 inch depth, and a clear span of 11.5 feet each loaded with two symmetric point loads. Each specimen was pretensioned. After applying the selection criteria and discarding specimens with intentional damage or quality issues, only one test was included in the database.

3.3 CRITERIA USED IN SELECTING BEAMS TO BE USED IN THIS STUDY

Tests selected had to satisfy the following selection criteria.

1. Simply supported members with symmetrically applied loading.
2. Concrete compressive strength greater than 3000 psi at the time of the test.
3. Bonded (prestressed or nonprestressed) reinforcement.
4. A decompression moment exceeding 50% of the cracking moment at the midspan cross section.
5. Members for which the maximum reasonable service-level moment at midspan exceeds the Class U limit.

The overall goal of this study is to look at a typical modern prestressed flexural member design. The selection criteria were adopted to filter out members that would not be expected to crack under service-level loads as well as those using out-of-date materials or construction methods. Criterion 2 was employed because modern prestressed concrete structural components do not have a strength less than 3000 psi. Criterion 3 was applied to exclude the complex behavior of unbonded prestressing and to filter out intentionally flawed specimens such as some in the study by Warwaruk (1960). This criterion also was put in place to not complicate the prediction of how the prestressing interacted with the concrete and not to have the difficulty of predicting the stress in the overall beam. Criterion 4 addresses any beams in older studies that could be disputed as a nonprestressed concrete beam or being lightly prestressed enough to be considered as a nonprestressed concrete beam since there is no defined boundary of how prestressed a beam must be to be considered prestressed in ACI 318. Criterion 5 was applied because most tests were not specifically designed with Class U, T, or C in mind because these classes did not necessarily exist at the time. In order to distinguish which beams could be considered as Class T or Class C, a maximum reasonable service-level moment ($M_{s,max}$) was determined for each test and was chosen as the least of three limiting values based on how each test was conducted. These three limiting values are as follows:

- 2/3 of the nominal moment strength, M_n
- 2/3 of the test failure moment, M_F
- The moment at which a shear crack was observed in the test, M_V

M_n was calculated assuming an equivalent rectangular concrete stress distribution in accordance with ACI 318 (2019) Section 22.2.2.3. An iterative strain compatibility analysis was used to determine the stress in the nonprestressed and prestressed reinforcement at this calculated M_n. Given ACI 318 load and strength-reduction factors, a service-level moment cannot exceed $(2/3)M_n$. This was the most commonly controlling maximum in the database, and it precludes most flexural tests of (“fully prestressed”) members reported in literature. Some of the older tests fractured before the specimen ever achieved $2/3M_n$, so the limiting moment was taken to be 2/3 of the actual failure moment (M_F) to more accurately limit the service-level moment for these beams. A few beams were specifically designed to fail in shear with a diverse range of partial prestressing techniques. It was judged that the maximum service-level moments for these specimens could not reasonably exceed the midspan bending moment at the onset of the first major shear crack, M_V, which was determined from the load reported by the study author(s).

3.4 DATABASE DATA PROVIDED

For each test in the database, the following information is listed in U.S. customary units:

- A reference ID number unique to this study

- Author(s) of original test report/article
- Identification code provided by original reporting author(s)
- Reported specimen and test geometry
    - Midspan Gross Cross-Sectional Geometry
        - Cross Section Type
        - h, b_f, h_f, b_w, $y_{t,gross}$
        - A_g, I_g (calculated if not reported)
- Material properties
    - Concrete properties
        - $f'_{c,test}$ - Compressive strength of the concrete at the time of the test
        - E_c - Modulus of elasticity of concrete
- Reinforcement properties
    - Type of reinforcement (pre/post-tensioned, nonprestressed tension, nonprestressed compression)
    - Diameter and area of prestressed reinforcement and nonprestressed reinforcement
    - Effective depth of prestressed reinforcement and nonprestressed reinforcement
    - Number of different sized nonprestressed reinforcement bars in flexural member
    - Length of nonprestressed reinforcement (L_s)
    - f_{pu}, f_y - Strength of prestressed and nonprestressed reinforcement
    - f_{ps} - Stress in the prestressed reinforcement at nominal flexural strength

    - $f_{pe,w}$ – Effective prestress in the prestressed reinforcement under self-weight
- Span and Loading Configuration of Applied Loads
    - Length of the entire beam (L_{Total})
    - Clear span between supports (L)
    - Number of point loads (0 if distribued load)
    - Location of point loads relative to nearest support

Material properties are values reported by original researchers. Some studies however did not report all values. In Shaikh (1967), an f'_c value at the time of testing was not reported so the best estimate for $f'_{c,test}$ was the reported 28-day compressive strength. When computing M_n, the f_{ps} values were estimated using equations reported in Design Aid 15.3.3 of the PCI Design Handbook 7th Ed. for a 250 ksi strand in Equation 3-1 and Equation 3-2 and 270 ksi strand in Equation 3-3 and Equation 3-4, respectively:

$$\varepsilon_{ps} \leq 0.0076\text{: } f_{ps} = 28{,}800\varepsilon_{ps}\ (ksi) \qquad \textit{Equation 3-1}$$

$$\varepsilon_{ps} > 0.0076\text{: } f_{ps} = 250 - \frac{0.04}{\varepsilon_{ps} - 0.0064}\ (ksi) \qquad \textit{Equation 3-2}$$

$$\varepsilon_{ps} \leq 0.0085\text{: } f_{ps} = 28{,}800\varepsilon_{ps}\ (ksi) \qquad \textit{Equation 3-3}$$

$$\varepsilon_{ps} > 0.0085\text{: } f_{ps} = 270 - \frac{0.04}{\varepsilon_{ps} - 0.007}\ (ksi) \qquad \textit{Equation 3-4}$$

For linear elastic (uncracked- and cracked-section) analyses, E_p of 28,500 ksi was used with the one exception of the Janney (1956) study that reported an E_p of 28,000 ksi. An assumption was made for the nonprestressed reinforcement to have an E_s of 29,000 ksi with no studies having reported this value. The modulus of elasticity of the concrete (E_c) is listed in the database as either a calculated or reported value. Calculated values are shown in the database in boldface. The majority of the values of $f_{pe,w}$ were reported either as a stress or as an effective prestress force that was back-calculated into a corresponding stress. The only exception is the Shaikh (1967) study, where measured change in concrete strain between time of prestressing and time of testing was used to calculate the effective prestress using the reported force in the strand before transfer and the change in the strain at the time of prestressing.

- Characteristics related to load-deflection response
  - Self-weight moment (M_w)
  - Decompression moment corresponding to zero stress at tension face as described in Section 2.3.1 (M_{dec})
  - Total midspan bending moment at each key service load level
  - $M_{s,max}$ (All three limiting values described in Section 3.3 are reported; the controlling value is in boldface italics.)
  - The classification (T or C) of the beam based on $M_{s,max}$
  - Reported deflections at each key service load level

3.5 KEY SERVICE LOAD LEVELS

Key service load levels were selected to enable direct numerical comparison of predicted and measured deflections through the range of service loads that might be expected for Class T and Class C members. These key service load levels were determined based on the computed tension stress in the extreme tension fiber of the concrete. The corresponding stress levels are as follows:

1. $6\sqrt{f'_c}$
2. $7.5\sqrt{f'_c}$
3. $10\sqrt{f'_c}$

4. $12\sqrt{f'_c}$
5. $M_{s,max}$

The first level is to investigate expected linear-elastic, uncracked behavior. The second level is the theoretical cracking point of the beam. This also is the boundary between Class U and Class T beam behavior. The third level is an intermediate point between the boundaries of Class T and Class C. This level shows any trends that may form as well as providing an intermediate datapoint for deflection of beams within the Class T zone. The fourth level falls at the boundary between Class T and Class C beams. The fifth level corresponds to the maximum reasonable service-level moment for which the specimen could have been designed. For a given specimen, this level may fall anywhere from Class U to Class C depending on the least of the three limiting M_s values described above. In addition to these key service load levels, the database also includes the total calculated bending moment that corresponds to an extreme compression fiber stress of $0.60f'_c$, $M_{TOTAL,0.6}$, which is the maximum permissible compressive stress for Class U and Class T members under service loads (ACI 318-19 Section 24.5.4.1).

For each test in the database, the deflection at each key service load level was carefully determined by enlarging and scaling the load versus deflection plots provided in the original test report/article.

CHAPTER 4: EVALUATING THE ACCURACY OF PREDICTION METHODS

4.1 INTRODUCTION

Four methods of predicting immediate deflection in prestressed concrete beams were compared to look at the conservatism and accuracy of each method comparatively to one another. This chapter provides the results of predictions using these methods and discusses the comparisons between the predictions and measured deflections and any inaccuracies resulting from each method. These four prediction methods are as follows:

- Branson I_e without influence of prestress force—uncracked section properties are applied for the portion of the deflection occurring up to the decompression moment (M_{dec}). For the portion of the deflection beyond M_{dec}, the Branson I_e as expressed in Equation 2-2 is applied, and I_{cr} does not include the influence of the prestress force (i.e., the "fully cracked" I_{cr}). These predictions are denoted as $\Delta_{B\ no\ P}$ or "Branson no P."
- Proposed Method (Branson I_e including influence of prestress force)—uncracked section properties are applied for the portion of the deflection occurring up to the decompression moment (M_{dec}). For the portion of the deflection beyond M_{dec}, the Branson I_e as expressed in Equation 2-2 is applied, and I_{cr} does include the influence of the prestress force (i.e., the "partially cracked" I_{cr}). These predictions are denoted as $\Delta_{Proposed}$.
- Rational Method—the Rational approach formulated by Bischoff, Naito, and Ingaglio (2018) and described in Section 2.3.3.
- Trilinear Method—the Trilinear approach formulated by Bischoff, Naito, and Ingaglio (2018) and described in Section 2.3.3.

4.2 RESULTS

Results for the four methods in the form of predicted and measured deflections at key service load levels are reported in Table 4-1 through Table 4-7. Each table contains a reference number and Beam ID that correspond to the database in Appendix C. Table 4-1, Table 4-2, and Table 4-3 include all forty beams determined to represent Class T members. Table 4-4, Table 4-5, Table 4-6, and Table 4-7 include all sixty-six beams determined to represent Class C members. Each group of tables is then broken down to include the moment, measured deflection and predicted deflections per method for the key service loading levels of $7.5\sqrt{f'_c}$, $10\sqrt{f'_c}$, $12\sqrt{f'_c}$, and maximum tension stress level for each beam. The Class T beams do not exceed the service loading level of $12\sqrt{f'_c}$ so this level is only included in the Class C results. In Table 4-1 and Table 4-4, the self-weight moment for each beam is also included. This moment was subtracted from the total moment at each load level to compare measured and predicted deflections at the applied loads reported in the literature without the effects of self-weight. A cell with "N/A" indicates that this load level exceeds the reasonable service-load range (greater than $M_{s,max}$) for the test.

Table 4-1: Measured and predicted deflections in Class T beams at $7.5\sqrt{f'_c}$ tension stress level

Ref #	Reference Author(s)	Beam ID	M_w (kip-in)	$M_{TOTAL,7.5}$ (kip-in)	$\Delta_{test,7.5}$ (in.)	$\Delta_{predict,7.5}$ (in.)
1	Naito,Cetisli, Tate	NR-12	10	114	0.38	0.24
6	Aswad et al.	DT-2	5138	10212	1.46	1.06
7	Aswad et al.	DT-3	5645	10188	0.76	0.77
8	Saqan, Frosch	V-4-0.93	110	2917	0.059	0.044
29	Warwaruk, Sozen	OB.24.189	9	245	0.13	0.09
30	Warwaruk, Sozen	OB.34.038	9	207	0.12	0.05
31	Warwaruk, Sozen	OB.34.043	9	186	0.16	0.05
33	Warwaruk, Sozen	OB.34.073	9	169	0.13	0.06
42	Warwaruk, Sozen	OB.34.200	9	326	0.19	0.11
43	Warwaruk, Sozen	OB.34.290	9	282	0.13	0.12
44	Warwaruk, Sozen	OB.44.140	9	380	0.21	0.11
45	Warwaruk, Sozen	OB.44.158	9	283	0.17	0.11
46	Warwaruk, Sozen	RB.34.093	9	198	0.14	0.07
47	Warwaruk, Sozen	RB.34.126	9	298	0.16	0.10
59	Sozen	A.12.60	9	306	0.17	0.13
68	Sozen	B.11.07	6	212	0.06	0.05
69	Sozen	B.11.20	6	228	0.08	0.07
70	Sozen	B.11.29	6	278	0.09	0.09
71	Sozen	B.12.12	6	193	0.15	0.07
72	Sozen	B.12.14	6	186	0.08	0.08
73	Sozen	B.12.26	6	254	0.16	0.10
75	Sozen	B.12.35	6	268	0.18	0.12
76	Sozen	B.13.16	6	243	0.13	0.09
79	Sozen	C.12.18	6	220	0.15	0.08
80	Sozen	C.12.19	6	272	0.12	0.09
81	Hernandez	G1	5	176	0.12	0.08
82	Hernandez	G2	5	177	0.13	0.08
83	Hernandez	G5	5	283	0.15	0.13
84	Hernandez	G7	5	294	0.17	0.11
85	Hernandez	G9	5	176	0.11	0.08
86	Hernandez	G11	5	177	0.09	0.08
88	Hernandez	G13	5	176	0.10	0.08
90	Hernandez	G16	6	278	0.16	0.12
92	Hernandez	G24	5	281	0.16	0.13
93	Hernandez	G25	5	178	0.10	0.08
96	Hernandez	G29	5	282	0.17	0.12
99	Hernandez	G35	6	280	0.14	0.10
100	Hernandez	G37	6	276	0.12	0.11
101	Janney et al.	1-0.141	9	163	0.07	0.05
104	Janney et al.	2-0.151	9	165	0.07	0.05

Table 4-2: Measured and predicted deflections in Class T beams at $10\sqrt{f'_c}$ tension stress level

Ref #	Beam ID	$M_{TOTAL,10}$ (kip-in)	$\Delta_{test,10}$ (in.)	$\Delta_{B\ no\ P,10}$ (in.)	$\Delta_{Proposed,10}$ (in.)	$\Delta_{Rational,10}$ (in.)	$\Delta_{Trilinear,10}$ (in.)
1	NR-12	N/A	N/A	N/A	N/A	N/A	N/A
6	DT-2	10701	1.76	1.57	1.56	1.99	1.82
7	DT-3	N/A	N/A	N/A	N/A	N/A	N/A
8	V-4-0.93	3352	0.076	0.076	0.076	0.108	0.116
29	OB.24.189	270	0.18	0.13	0.13	0.15	0.14
30	OB.34.038	N/A	N/A	N/A	N/A	N/A	N/A
31	OB.34.043	N/A	N/A	N/A	N/A	N/A	N/A
33	OB.34.073	N/A	N/A	N/A	N/A	N/A	N/A
42	OB.34.200	352	0.23	0.16	0.15	0.15	0.16
43	OB.34.290	N/A	N/A	N/A	N/A	N/A	N/A
44	OB.44.140	N/A	N/A	N/A	N/A	N/A	N/A
45	OB.44.158	N/A	N/A	N/A	N/A	N/A	N/A
46	RB.34.093	N/A	N/A	N/A	N/A	N/A	N/A
47	RB.34.126	325	0.20	0.15	0.14	0.16	0.15
59	A.12.60	N/A	N/A	N/A	N/A	N/A	N/A
68	B.11.07	N/A	N/A	N/A	N/A	N/A	N/A
69	B.11.20	251	0.10	0.11	0.11	0.15	0.14
70	B.11.29	300	0.10	0.12	0.12	0.14	0.13
71	B.12.12	N/A	N/A	N/A	N/A	N/A	N/A
72	B.12.14	N/A	N/A	N/A	N/A	N/A	N/A
73	B.12.26	N/A	N/A	N/A	N/A	N/A	N/A
75	B.12.35	N/A	N/A	N/A	N/A	N/A	N/A
76	B.13.16	N/A	N/A	N/A	N/A	N/A	N/A
79	C.12.18	N/A	N/A	N/A	N/A	N/A	N/A
80	C.12.19	N/A	N/A	N/A	N/A	N/A	N/A
81	G1	N/A	N/A	N/A	N/A	N/A	N/A
82	G2	N/A	N/A	N/A	N/A	N/A	N/A
83	G5	303	0.16	0.17	0.17	0.19	0.18
84	G7	317	0.20	0.16	0.16	0.19	0.18
85	G9	N/A	N/A	N/A	N/A	N/A	N/A
86	G11	N/A	N/A	N/A	N/A	N/A	N/A
88	G13	N/A	N/A	N/A	N/A	N/A	N/A
90	G16	N/A	N/A	N/A	N/A	N/A	N/A
92	G24	301	0.20	0.17	0.17	0.19	0.18
93	G25	N/A	N/A	N/A	N/A	N/A	N/A
96	G29	N/A	N/A	N/A	N/A	N/A	N/A
99	G35	301	0.16	0.14	0.14	0.15	0.15
100	G37	297	0.15	0.14	0.14	0.16	0.15
101	1-0.141	189	0.08	0.10	0.10	0.26	0.26
104	2-0.151	191	0.12	0.11	0.11	0.25	0.25

Table 4-3: Measured and predicted deflections in Class T beams at maximum tension stress level

Ref #	Beam ID	$M_{s,max}$ (kip-in)	Δ_{max} (in.)	$\Delta_{B\ no\ P,max}$ (in.)	$\Delta_{Proposed,max}$ (in.)	$\Delta_{Rational,max}$ (in.)	$\Delta_{Trilinear,max}$ (in.)
1	NR-12	123	0.43	0.34	0.33	0.44	0.43
6	DT-2	10789	1.85	1.87	1.67	2.13	1.96
7	DT-3	10392	0.81	1.01	0.91	1.25	1.12
8	V-4-0.93	3432	0.082	0.084	0.083	0.118	0.129
29	OB.24.189	277	0.18	0.15	0.14	0.16	0.16
30	OB.34.038	236	0.20	0.10	0.10	0.23	0.24
31	OB.34.043	194	0.20	0.06	0.06	0.12	0.11
33	OB.34.073	180	0.16	0.08	0.08	0.14	0.13
42	OB.34.200	372	0.26	0.20	0.18	0.18	0.19
43	OB.34.290	294	0.15	0.14	0.13	0.14	0.14
44	OB.44.140	401	0.23	0.14	0.14	0.14	0.15
45	OB.44.158	294	0.20	0.13	0.12	0.13	0.13
46	RB.34.093	217	0.18	0.11	0.11	0.16	0.15
47	RB.34.126	334	0.21	0.17	0.16	0.18	0.17
59	A.12.60	328	0.19	0.17	0.16	0.16	0.17
68	B.11.07	215	0.06	0.05	0.05	0.06	0.06
69	B.11.20	251	0.10	0.11	0.11	0.15	0.14
70	B.11.29	316	0.12	0.16	0.15	0.17	0.17
71	B.12.12	209	0.20	0.10	0.10	0.16	0.17
72	B.12.14	207	0.16	0.12	0.12	0.19	0.20
73	B.12.26	276	0.21	0.14	0.13	0.17	0.16
75	B.12.35	278	0.20	0.13	0.13	0.15	0.14
76	B.13.16	254	0.16	0.11	0.11	0.15	0.14
79	C.12.18	222	0.15	0.08	0.08	0.09	0.09
80	C.12.19	274	0.15	0.09	0.09	0.10	0.10
81	G1	190	0.17	0.11	0.11	0.17	0.18
82	G2	191	0.17	0.11	0.11	0.17	0.18
83	G5	310	0.18	0.19	0.19	0.21	0.20
84	G7	331	0.22	0.19	0.19	0.23	0.22
85	G9	189	0.16	0.11	0.11	0.17	0.18
86	G11	189	0.15	0.11	0.11	0.17	0.17
88	G13	189	0.14	0.11	0.11	0.17	0.17
90	G16	293	0.20	0.14	0.14	0.16	0.15
92	G24	312	0.23	0.20	0.20	0.22	0.21
93	G25	190	0.15	0.11	0.11	0.16	0.17
96	G29	283	0.18	0.12	0.12	0.12	0.12
99	G35	315	0.20	0.18	0.17	0.18	0.18
100	G37	313	0.19	0.18	0.18	0.19	0.18
101	1-0.141	198	0.09	0.13	0.13	0.31	0.34
104	2-0.151	197	0.15	0.13	0.12	0.29	0.29

Table 4-4: Measured and predicted deflections in Class C beams at $7.5\sqrt{f'_c}$ tension stress level

Ref #	Reference Author(s)	Beam ID	M_w (kip-in)	$M_{TOTAL,7.5}$ (kip-in)	$\Delta_{test,7.5}$ (in.)	$\Delta_{predict,7.5}$ (in.)
2	Brewe, Myers	B-84	22	703	0.44	0.47
3	Brewe, Myers	B-75	24	705	0.41	0.44
4	Brewe, Myers	B-68	26	688	0.38	0.39
5	Aswad et al.	DT-1	5473	10515	0.95	0.96
9	Saqan, Frosch	V-4-2.37	112	2995	0.054	0.043
10	Saqan, Frosch	V-7-0	107	2935	0.058	0.045
11	Saqan, Frosch	V-7-1.84	108	3006	0.050	0.044
12	Saqan, Frosch	V-7-2.37	106	3004	0.050	0.045
13	Saqan, Frosch	V-10-0	108	2966	0.064	0.046
14	Saqan, Frosch	V-10-1.51	108	3025	0.055	0.045
15	Saqan, Frosch	V-10-2.37	108	3057	0.052	0.045
16	Shaikh	Series I.1	17	129	0.41	0.34
17	Shaikh	Series I.2	17	125	0.38	0.32
18	Shaikh	Series I.3	17	129	0.41	0.33
19	Shaikh	Series II.1	17	102	0.23	0.25
20	Shaikh	Series II.2	17	103	0.25	0.25
21	Shaikh	Series II.3	17	102	0.26	0.24
22	Shaikh	Series III.1	17	127	0.40	0.30
23	Shaikh	Series III.2	17	133	0.34	0.32
24	Shaikh	Series III.3	17	127	0.31	0.30
25	Shaikh	Series IV.1	17	115	0.26	0.28
26	Shaikh	Series IV.2	17	117	0.29	0.28
27	Shaikh	Series IV.3	17	113	0.28	0.27
28	Warwaruk, Sozen	OB.24.168	9	192	0.11	0.07
32	Warwaruk, Sozen	OB.34.071	9	282	0.13	0.08
34	Warwaruk, Sozen	OB.34.074	9	288	0.17	0.08
35	Warwaruk, Sozen	OB.34.076	9	213	0.11	0.07
36	Warwaruk, Sozen	OB.34.077	9	241	0.11	0.07
37	Warwaruk, Sozen	OB.34.115	9	337	0.20	0.09
38	Warwaruk, Sozen	OB.34.120	9	208	0.07	0.08
39	Warwaruk, Sozen	OB.34.122	9	277	0.16	0.09
40	Warwaruk, Sozen	OB.34.159	9	308	0.13	0.09
41	Warwaruk, Sozen	OB.34.196	9	211	0.10	0.09

Table 4-4: Measured and predicted deflections in Class C beams at $7.5\sqrt{f'_c}$ tension stress level (Cont.)

Ref #	Reference Author(s)	Beam ID	M_w (kip-in)	$M_{TOTAL,7.5}$ (kip-in)	$\Delta_{test,7.5}$ (in.)	$\Delta_{predict,7.5}$ (in.)
48	Sozen	A.11.43	9	311	0.09	0.07
49	Sozen	A.11.53	9	265	0.08	0.08
50	Sozen	A.12.23	9	241	0.11	0.08
51	Sozen	A.12.31	9	254	0.16	0.08
52	Sozen	A.12.34	9	308	0.13	0.08
53	Sozen	A.12.36	9	209	0.09	0.08
54	Sozen	A.12.42	9	290	0.15	0.09
55	Sozen	A.12.46	9	275	0.15	0.10
56	Sozen	A.12.48	9	308	0.16	0.11
57	Sozen	A.12.53	9	226	0.10	0.09
58	Sozen	A.12.56	9	277	0.15	0.11
60	Sozen	A.12.73	9	280	0.16	0.11
61	Sozen	A.14.39	4	177	0.05	0.05
62	Sozen	A.14.44	4	200	0.04	0.05
63	Sozen	A.14.55	4	235	0.04	0.06
64	Sozen	A.21.39	9	128	0.05	0.04
65	Sozen	A.21.51	9	201	0.05	0.05
66	Sozen	A.22.40	9	202	0.11	0.06
67	Sozen	A.22.49	9	170	0.08	0.06
74	Sozen	B.12.29	6	264	0.18	0.11
77	Sozen	B.21.26	6	179	0.06	0.05
78	Sozen	B.22.23	6	169	0.11	0.06
87	Hernandez	G12	6	272	0.15	0.13
89	Hernandez	G14	6	271	0.13	0.12
91	Hernandez	G22	5	268	0.17	0.12
94	Hernandez	G27	5	296	0.14	0.11
95	Hernandez	G28	6	267	0.18	0.11
97	Hernandez	G30	6	284	0.13	0.10
98	Hernandez	G31	6	272	0.10	0.10
102	Janney et al.	1-0.250	9	245	0.09	0.07
103	Janney et al.	1-0.420	9	333	0.13	0.11
105	Janney et al.	2-0.306	9	244	0.10	0.08
106	Janney et al.	2-0.398	9	335	0.14	0.10

Table 4-5: Measured and predicted deflections in Class C beams at $10\sqrt{f'_c}$ tension stress level

Ref #	Beam ID	$M_{TOTAL,10}$ (kip-in)	$\Delta_{test,10}$ (in.)	$\Delta_{B\ no\ P,10}$ (in.)	$\Delta_{Proposed,10}$ (in.)	$\Delta_{Rational,10}$ (in.)	$\Delta_{Trilinear,10}$ (in.)
2	B-84	733	0.46	0.56	0.53	0.53	0.55
3	B-75	737	0.44	0.53	0.50	0.50	0.51
4	B-68	723	0.40	0.49	0.46	0.46	0.48
5	DT-1	11082	1.32	1.52	1.51	2.14	1.96
9	V-4-2.37	3459	0.070	0.070	0.070	0.081	0.086
10	V-7-0	3357	0.082	0.081	0.081	0.143	0.152
11	V-7-1.84	3454	0.063	0.072	0.071	0.083	0.088
12	V-7-2.37	3452	0.063	0.070	0.070	0.078	0.082
13	V-10-0	3386	0.082	0.080	0.079	0.117	0.124
14	V-10-1.51	3467	0.070	0.072	0.072	0.083	0.087
15	V-10-2.37	3512	0.062	0.070	0.069	0.075	0.080
16	Series I.1	141	0.47	0.50	0.49	0.53	0.52
17	Series I.2	137	0.45	0.47	0.46	0.50	0.49
18	Series I.3	142	0.46	0.47	0.47	0.49	0.49
19	Series II.1	115	0.30	0.43	0.43	0.62	0.61
20	Series II.2	116	0.32	0.41	0.40	0.49	0.49
21	Series II.3	116	0.34	0.39	0.39	0.44	0.46
22	Series III.1	141	0.46	0.45	0.44	0.49	0.49
23	Series III.2	147	0.41	0.51	0.50	0.64	0.60
24	Series III.3	140	0.34	0.47	0.47	0.56	0.54
25	Series IV.1	128	0.30	0.45	0.45	0.55	0.53
26	Series IV.2	130	0.36	0.42	0.42	0.45	0.45
27	Series IV.3	127	0.34	0.41	0.40	0.43	0.44
28	OB.24.168	214	0.14	0.12	0.12	0.15	0.15
32	OB.34.071	314	0.18	0.13	0.13	0.16	0.16
34	OB.34.074	322	0.24	0.13	0.12	0.16	0.16
35	OB.34.076	241	0.13	0.12	0.12	0.18	0.17
36	OB.34.077	270	0.15	0.12	0.12	0.17	0.16
37	OB.34.115	370	0.23	0.14	0.13	0.15	0.15
38	OB.34.120	231	0.09	0.13	0.13	0.16	0.15
39	OB.34.122	306	0.20	0.13	0.13	0.15	0.15
40	OB.34.159	337	0.16	0.14	0.13	0.15	0.15
41	OB.34.196	232	0.13	0.14	0.13	0.15	0.15

Table 4-5: Measured and predicted deflections in Class C beams at $10\sqrt{f'_c}$ tension stress level (Cont.)

Ref #	Beam ID	$M_{TOTAL,10}$ (kip-in)	$\Delta_{test,10}$ (in.)	$\Delta_{B\ no\ P,10}$ (in.)	$\Delta_{Proposed,10}$ (in.)	$\Delta_{Rational,10}$ (in.)	$\Delta_{Trilinear,10}$ (in.)
48	A.11.43	340	0.10	0.11	0.10	0.12	0.12
49	A.11.53	289	0.10	0.11	0.11	0.11	0.12
50	A.12.23	270	0.13	0.12	0.12	0.17	0.16
51	A.12.31	282	0.21	0.13	0.12	0.16	0.15
52	A.12.34	341	0.16	0.13	0.13	0.15	0.15
53	A.12.36	231	0.12	0.13	0.13	0.16	0.15
54	A.12.42	319	0.19	0.13	0.13	0.15	0.14
55	A.12.46	301	0.16	0.14	0.14	0.15	0.15
56	A.12.48	334	0.18	0.15	0.14	0.15	0.16
57	A.12.53	247	0.13	0.14	0.13	0.15	0.14
58	A.12.56	300	0.17	0.15	0.14	0.15	0.15
60	A.12.73	303	0.18	0.15	0.15	0.15	0.15
61	A.14.39	198	0.08	0.08	0.08	0.11	0.10
62	A.14.44	221	0.06	0.08	0.08	0.10	0.10
63	A.14.55	257	0.06	0.09	0.09	0.10	0.10
64	A.21.39	148	0.07	0.08	0.08	0.13	0.14
65	A.21.51	228	0.07	0.08	0.08	0.11	0.11
66	A.22.40	230	0.13	0.11	0.11	0.16	0.15
67	A.22.49	195	0.11	0.10	0.10	0.15	0.15
74	B.12.29	287	0.20	0.15	0.15	0.18	0.17
77	B.21.26	203	0.08	0.09	0.09	0.12	0.13
78	B.22.23	194	0.17	0.10	0.10	0.16	0.18
87	G12	291	0.17	0.17	0.17	0.18	0.17
89	G14	291	0.16	0.17	0.16	0.18	0.17
91	G22	288	0.21	0.16	0.16	0.19	0.18
94	G27	320	0.18	0.15	0.15	0.19	0.18
95	G28	289	0.24	0.15	0.15	0.18	0.17
97	G30	310	0.18	0.14	0.14	0.18	0.17
98	G31	292	0.12	0.13	0.13	0.14	0.14
102	1-0.250	273	0.11	0.12	0.12	0.16	0.15
103	1-0.420	360	0.16	0.15	0.14	0.15	0.15
105	2-0.306	270	0.11	0.13	0.13	0.15	0.15
106	2-0.398	363	0.17	0.15	0.14	0.15	0.15

Table 4-6: Measured and predicted deflections in Class C beams at $12\sqrt{f'_c}$ tension stress level

Ref #	Beam ID	$M_{TOTAL,12}$ (kip-in)	$\Delta_{test,12}$ (in.)	$\Delta_{B\ no\ P,12}$ (in.)	$\Delta_{Proposed,12}$ (in.)	$\Delta_{Rational,12}$ (in.)	$\Delta_{Trilinear,12}$ (in.)
2	B-84	757	0.48	0.66	0.59	0.58	0.60
3	B-75	764	0.46	0.63	0.56	0.55	0.58
4	B-68	752	0.42	0.59	0.53	0.52	0.55
5	DT-1	11535	1.74	2.52	2.19	2.94	2.76
9	V-4-2.37	3831	0.086	0.096	0.096	0.106	0.121
10	V-7-0	3694	0.117	0.125	0.125	0.207	0.237
11	V-7-1.84	3812	0.078	0.098	0.098	0.108	0.122
12	V-7-2.37	3810	0.076	0.094	0.094	0.100	0.112
13	V-10-0	3721	0.101	0.118	0.118	0.164	0.186
14	V-10-1.51	3821	0.086	0.099	0.098	0.108	0.121
15	V-10-2.37	3876	0.073	0.092	0.092	0.096	0.107
16	Series I.1	151	0.55	0.67	0.65	0.68	0.67
17	Series I.2	147	0.51	0.62	0.60	0.63	0.63
18	Series I.3	152	0.53	0.60	0.59	0.60	0.61
19	Series II.1	125	0.39	0.65	0.64	0.87	0.89
20	Series II.2	126	0.42	0.57	0.57	0.64	0.69
21	Series II.3	126	0.44	0.54	0.53	0.57	0.63
22	Series III.1	152	0.54	0.60	0.59	0.63	0.65
23	Series III.2	157	0.53	0.73	0.71	0.87	0.83
24	Series III.3	151	0.41	0.67	0.65	0.74	0.73
25	Series IV.1	138	0.35	0.64	0.63	0.73	0.72
26	Series IV.2	141	0.42	0.56	0.55	0.57	0.59
27	Series IV.3	137	0.40	0.53	0.52	0.54	0.57
28	OB.24.168	233	0.22	0.18	0.17	0.21	0.20
32	OB.34.071	340	0.23	0.19	0.18	0.23	0.22
34	OB.34.074	348	0.29	0.18	0.18	0.23	0.22
35	OB.34.076	263	0.20	0.18	0.18	0.26	0.25
36	OB.34.077	293	0.19	0.18	0.18	0.24	0.23
37	OB.34.115	397	0.27	0.19	0.18	0.20	0.20
38	OB.34.120	249	0.14	0.18	0.18	0.22	0.21
39	OB.34.122	330	0.25	0.19	0.18	0.21	0.20
40	OB.34.159	361	0.20	0.19	0.18	0.19	0.19
41	OB.34.196	249	0.15	0.19	0.18	0.20	0.19

Table 4-6: Measured and predicted deflections in Class C beams at $12\sqrt{f'_c}$ tension stress level (Cont.)

Ref #	Beam ID	$M_{TOTAL,12}$ (kip-in)	$\Delta_{test,12}$ (in.)	$\Delta_{B\ no\ P,12}$ (in.)	$\Delta_{Proposed,12}$ (in.)	$\Delta_{Rational,12}$ (in.)	$\Delta_{Trilinear,12}$ (in.)
48	A.11.43	363	0.11	0.15	0.14	0.15	0.15
49	A.11.53	309	0.12	0.15	0.14	0.15	0.15
50	A.12.23	292	0.15	0.18	0.18	0.23	0.23
51	A.12.31	304	0.23	0.18	0.18	0.22	0.21
52	A.12.34	367	0.20	0.19	0.18	0.20	0.20
53	A.12.36	249	0.14	0.18	0.18	0.21	0.20
54	A.12.42	343	0.22	0.19	0.18	0.19	0.19
55	A.12.46	321	0.18	0.20	0.18	0.19	0.20
56	A.12.48	354	0.20	0.21	0.19	0.19	0.20
57	A.12.53	265	0.16	0.19	0.18	0.19	0.19
58	A.12.56	319	0.20	0.20	0.19	0.19	0.19
60	A.12.73	320	0.21	0.20	0.18	0.18	0.18
61	A.14.39	215	0.11	0.12	0.11	0.15	0.14
62	A.14.44	238	0.08	0.12	0.11	0.13	0.13
63	A.14.55	274	0.08	0.12	0.12	0.12	0.12
64	A.21.39	165	0.10	0.12	0.12	0.18	0.21
65	A.21.51	250	0.09	0.13	0.12	0.16	0.16
66	A.22.40	253	0.16	0.17	0.16	0.22	0.22
67	A.22.49	216	0.15	0.16	0.16	0.21	0.23
74	B.12.29	305	0.23	0.20	0.20	0.23	0.22
77	B.21.26	222	0.10	0.13	0.13	0.17	0.20
78	B.22.23	214	0.25	0.16	0.16	0.22	0.27
87	G12	307	0.20	0.21	0.21	0.22	0.21
89	G14	307	0.19	0.21	0.21	0.22	0.21
91	G22	304	0.25	0.21	0.21	0.23	0.22
94	G27	340	0.23	0.20	0.20	0.24	0.24
95	G28	307	0.26	0.20	0.20	0.22	0.21
97	G30	331	0.22	0.20	0.19	0.23	0.23
98	G31	309	0.15	0.17	0.16	0.17	0.17
102	1-0.250	296	0.14	0.18	0.18	0.23	0.21
103	1-0.420	382	0.18	0.20	0.18	0.18	0.19
105	2-0.306	291	0.17	0.19	0.18	0.21	0.20
106	2-0.398	385	0.19	0.20	0.18	0.18	0.19

Table 4-7: Measured and predicted deflections in Class C beams at maximum tension stress level

Ref #	Beam ID	$M_{s,max}$ (kip-in)	Δ_{max} (in.)	$\Delta_{B\ no\ P,max}$ (in.)	$\Delta_{Proposed,max}$ (in.)	$\Delta_{Rational,max}$ (in.)	$\Delta_{Trilinear,max}$ (in.)
2	B-84	848	0.60	1.04	0.91	0.77	0.82
3	B-75	871	0.61	1.07	0.94	0.77	0.83
4	B-68	884	0.56	1.13	1.02	0.81	0.86
5	DT-1	11843	2.08	3.20	2.75	3.47	3.31
9	V-4-2.37	4525	0.133	0.148	0.147	0.149	0.160
10	V-7-0	4269	0.238	0.226	0.226	0.305	0.326
11	V-7-1.84	5350	0.215	0.214	0.213	0.205	0.212
12	V-7-2.37	4865	0.137	0.164	0.164	0.159	0.166
13	V-10-0	4975	0.301	0.303	0.302	0.318	0.329
14	V-10-1.51	5397	0.205	0.216	0.215	0.206	0.213
15	V-10-2.37	5264	0.144	0.175	0.174	0.167	0.173
16	Series I.1	175	0.84	1.14	1.11	1.03	1.03
17	Series I.2	188	0.92	1.23	1.21	1.10	1.11
18	Series I.3	201	1.06	1.20	1.19	1.08	1.09
19	Series II.1	160	0.94	1.61	1.60	1.65	1.67
20	Series II.2	157	0.80	1.10	1.09	1.06	1.09
21	Series II.3	155	0.81	0.94	0.93	0.91	0.94
22	Series III.1	226	1.38	1.60	1.59	1.44	1.45
23	Series III.2	165	0.64	0.93	0.90	1.03	0.99
24	Series III.3	211	1.15	1.95	1.93	1.74	1.74
25	Series IV.1	193	1.00	1.82	1.80	1.65	1.66
26	Series IV.2	209	1.15	1.37	1.36	1.24	1.25
27	Series IV.3	201	1.08	1.20	1.20	1.11	1.12
28	OB.24.168	247	0.25	0.23	0.23	0.26	0.25
32	OB.34.071	359	0.26	0.24	0.23	0.27	0.27
34	OB.34.074	376	0.34	0.26	0.25	0.29	0.29
35	OB.34.076	281	0.25	0.24	0.24	0.32	0.32
36	OB.34.077	315	0.23	0.25	0.25	0.30	0.30
37	OB.34.115	446	0.35	0.32	0.31	0.29	0.28
38	OB.34.120	251	0.12	0.19	0.19	0.23	0.21
39	OB.34.122	364	0.33	0.30	0.28	0.29	0.28
40	OB.34.159	408	0.28	0.33	0.31	0.27	0.27
41	OB.34.196	254	0.16	0.21	0.20	0.21	0.21

Table 4-7: Measured and predicted deflections in Class C beams at maximum tension stress level (Cont.)

Ref #	Beam ID	$M_{s,max}$ (kip-in)	Δ_{max} (in.)	$\Delta_{B\ no\ P,max}$ (in.)	$\Delta_{Proposed,max}$ (in.)	$\Delta_{Rational,max}$ (in.)	$\Delta_{Trilinear,max}$ (in.)
48	A.11.43	424	0.16	0.29	0.27	0.24	0.23
49	A.11.53	327	0.14	0.20	0.18	0.17	0.18
50	A.12.23	331	0.22	0.31	0.30	0.34	0.34
51	A.12.31	326	0.29	0.25	0.24	0.27	0.26
52	A.12.34	405	0.29	0.29	0.27	0.28	0.27
53	A.12.36	266	0.17	0.25	0.24	0.27	0.26
54	A.12.42	379	0.27	0.29	0.27	0.26	0.25
55	A.12.46	337	0.20	0.25	0.23	0.22	0.23
56	A.12.48	367	0.21	0.24	0.22	0.21	0.22
57	A.12.53	285	0.20	0.26	0.25	0.24	0.24
58	A.12.56	324	0.21	0.22	0.20	0.20	0.20
60	A.12.73	323	0.20	0.21	0.19	0.18	0.19
61	A.14.39	231	0.14	0.16	0.15	0.19	0.18
62	A.14.44	256	0.10	0.16	0.16	0.17	0.16
63	A.14.55	283	0.09	0.14	0.13	0.13	0.13
64	A.21.39	203	0.21	0.25	0.25	0.30	0.32
65	A.21.51	318	0.17	0.28	0.27	0.28	0.28
66	A.22.40	321	0.29	0.38	0.38	0.40	0.40
67	A.22.49	284	0.33	0.39	0.38	0.40	0.41
74	B.12.29	309	0.23	0.21	0.21	0.24	0.23
77	B.21.26	228	0.12	0.14	0.14	0.18	0.21
78	B.22.23	230	0.32	0.20	0.20	0.27	0.31
87	G12	311	0.21	0.23	0.22	0.23	0.22
89	G14	314	0.20	0.23	0.23	0.24	0.23
91	G22	317	0.29	0.25	0.25	0.26	0.26
94	G27	342	0.24	0.21	0.21	0.25	0.24
95	G28	318	0.29	0.24	0.23	0.25	0.25
97	G30	340	0.24	0.22	0.22	0.26	0.25
98	G31	313	0.15	0.18	0.17	0.18	0.18
102	1-0.250	354	0.24	0.38	0.37	0.38	0.37
103	1-0.420	421	0.23	0.31	0.28	0.25	0.25
105	2-0.306	334	0.30	0.34	0.33	0.32	0.31
106	2-0.398	432	0.25	0.33	0.30	0.26	0.26

4.3 DISCUSSION

Figure 4-1 through Figure 4-3 show the four methods compared in this study for any beams that reached $10\sqrt{f'_c}$, $12\sqrt{f'_c}$, and the maximum reasonable service-level stress in histogram format. In each histogram, the ratio of predicted deflection versus measured deflection is on the horizontal axis while the relative frequency is displayed on the vertical axis. Figure 4-4 and Figure 4-5 are also histograms and show the accuracy of predictions at the maximum service-level stresses for Class T and Class C beams, respectively.

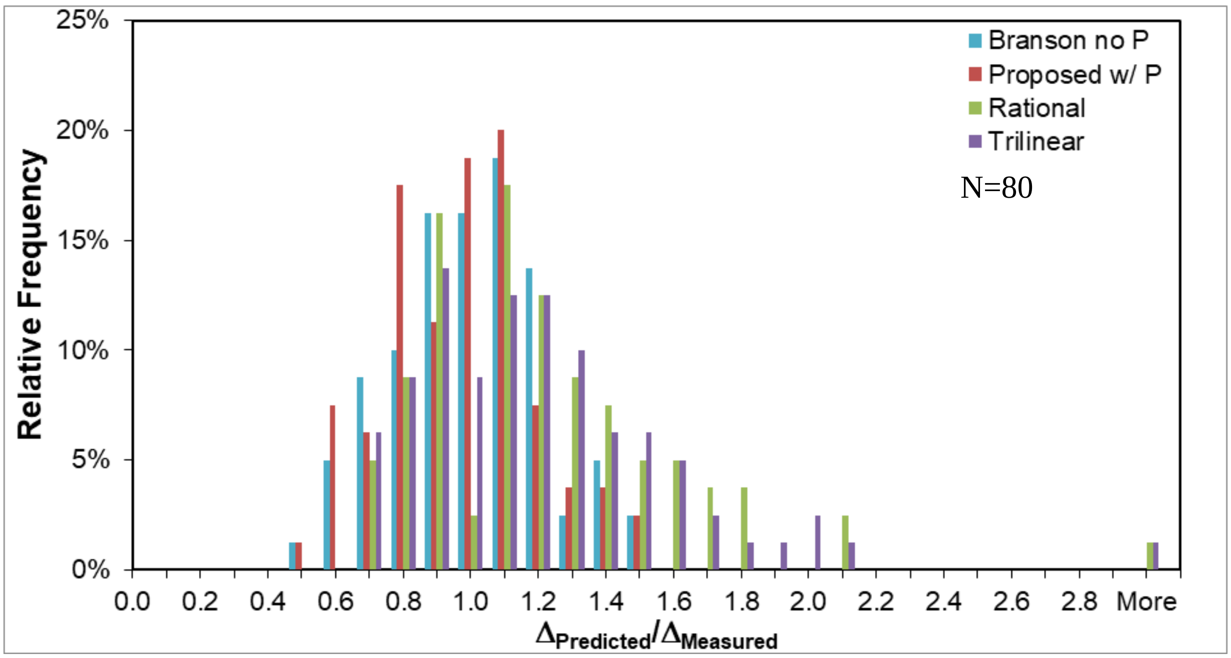

Figure 4-1: Comparison of prediction methods at a tension stress level of $10\sqrt{f'_c}$.

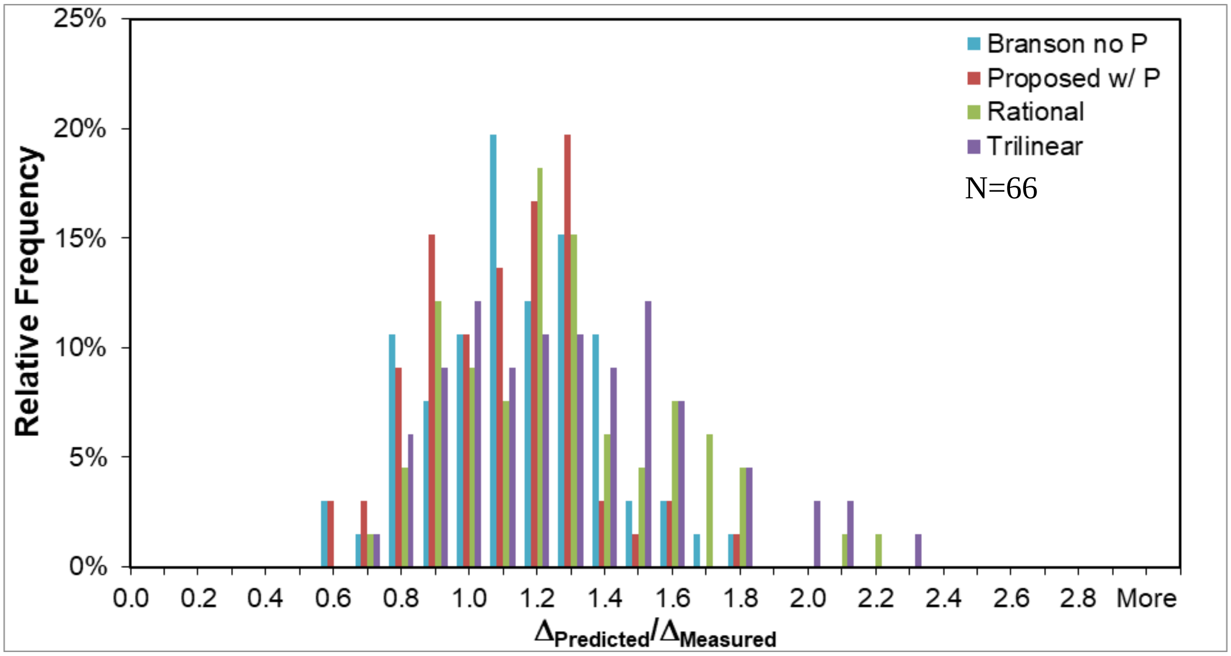

Figure 4-2: Comparison of prediction methods at a tension stress level of $12\sqrt{f'_c}$.

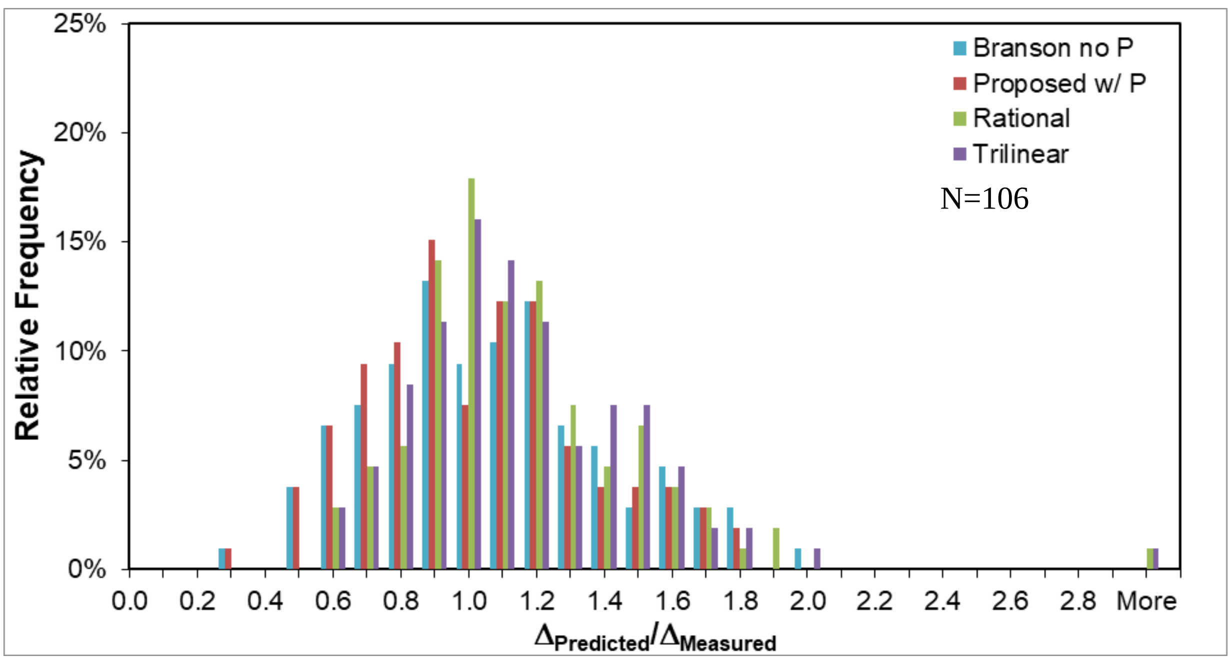

Figure 4-3: Comparison of prediction methods at the maximum reasonable service-level load.

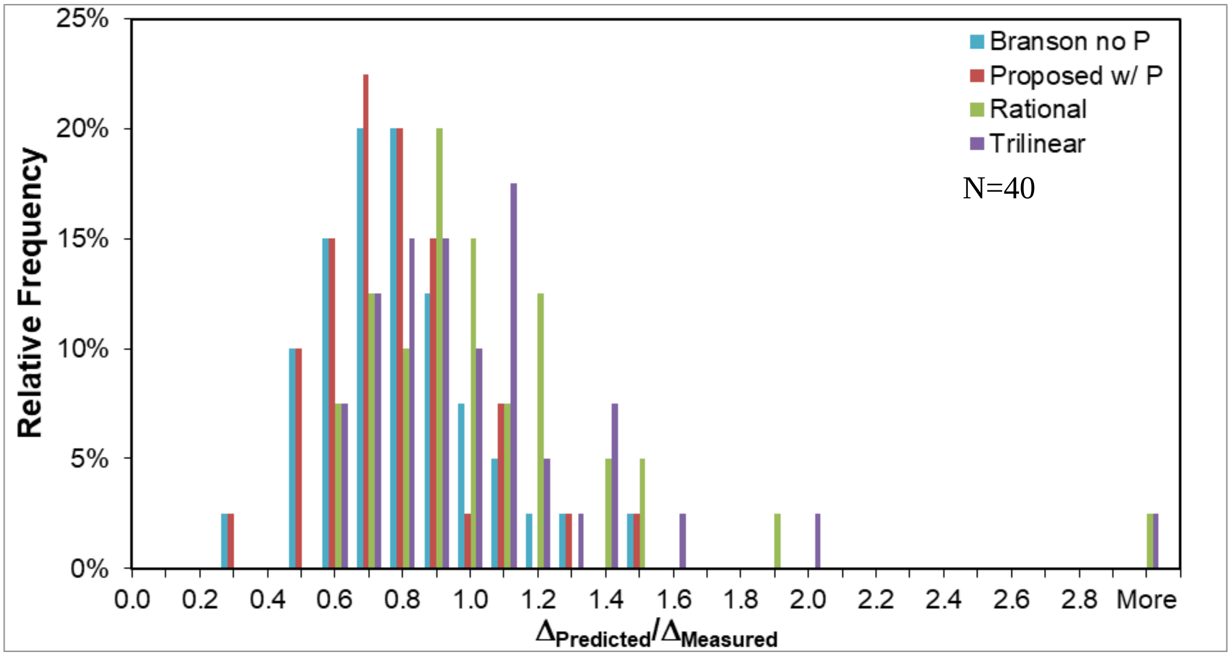

Figure 4-4: Comparison of prediction methods used for Class T members at the maximum reasonable service-level load.

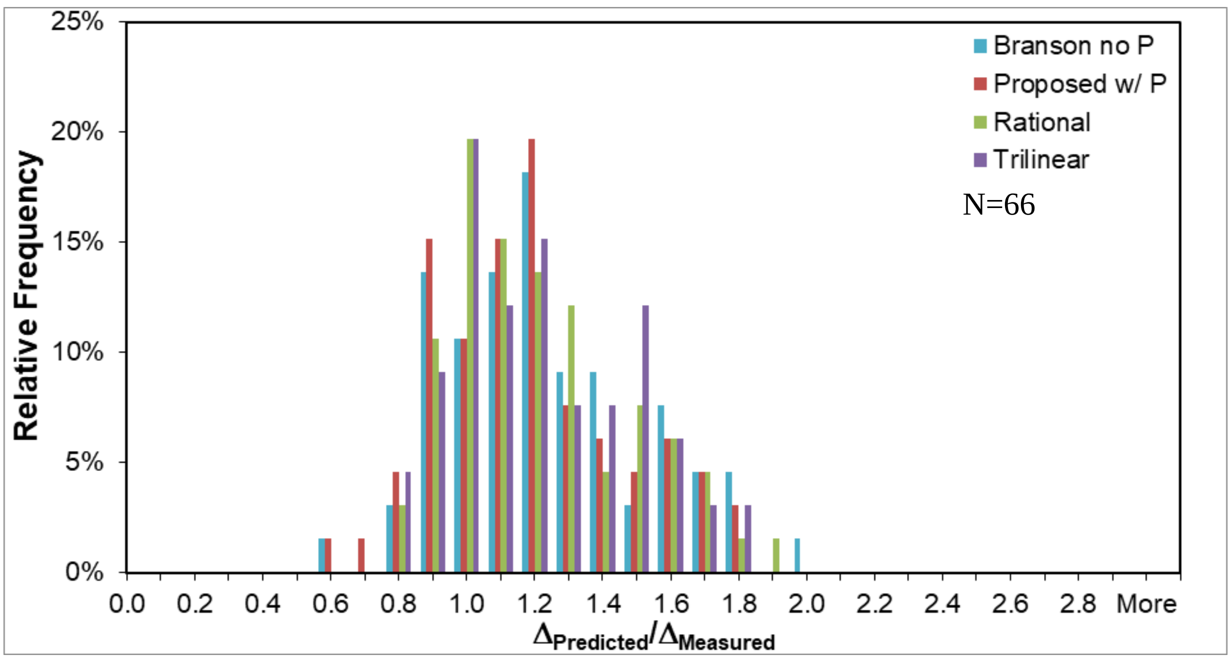

Figure 4-5: Comparison of prediction methods used for Class C members at the maximum reasonable service-level load.

Figure 4-6 is a box and whisker chart. Each box shows the quartile 1 and quartile 3 as the bottom and top, respectively, lines of the box with the median reported as a value and the black line cutting the box in two. When calculating the quartiles, the exclusive median method was used. This means the median was not included when finding the quartile ranges. The whiskers, which are the vertical black lines above and below the box, illustrate the entire range except extreme values. Any data more extreme than 1.5 times the interquartile range beyond the box were designated as extreme prediction values. These extreme values are shown as single points beyond the whiskers. Figure 4-6 shows three groupings of box and whiskers: deflections at $10\sqrt{f'_c}$, at $12\sqrt{f'_c}$, and at maximum service-level stress levels. The number of beams that reached each stress level is reported below each group. All four prediction methods are illustrated within each grouping.

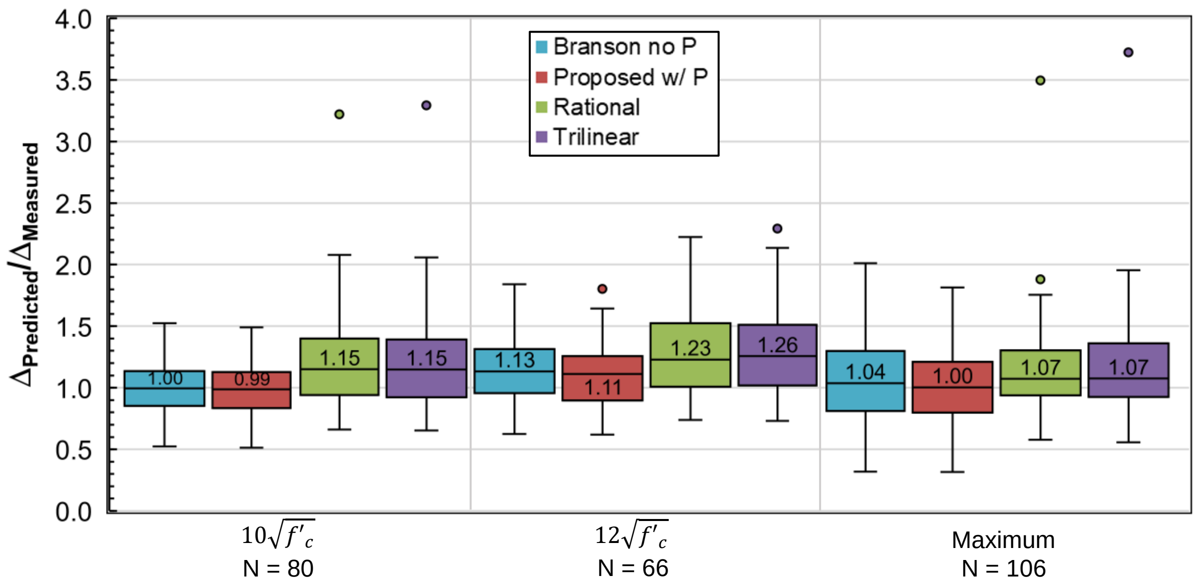

Figure 4-6: Distribution of prediction accuracy at key service load levels

When considering the eighty specimens that achieved $10\sqrt{f'_c}$, the two Branson I_e methods exhibit the best overall accuracy and least dispersion at that load level, with half of the predictions within $^+$/-15%. The Rational and Trilinear Methods resulted in more conservative predictions on average with a greater dispersion of accuracy. When considering the sixty-six specimens that achieved $12\sqrt{f'_c}$, the same overall relative comparison behavior of the four methods is evident; however, all methods exhibited an increase in conservatism on average. The

Proposed Method is the most accurate with the least dispersion at that load level. When considering the full database at the maximum service-level load for each specimen, the accuracy of all four methods is relatively good on average, with the Proposed Method as the most accurate with about half the predictions within $^{+}$/- 20%. Just as in the $10\sqrt{f'_c}$ results, the Rational and Trilinear Methods produced extreme overpredictions. The extreme overpredictions represented in Figure 4-6 ended up being for the same flexural member: Reference Number 101.

The Reference Number 101 specimen, a Class T beam that had very high prediction ratios for the Rational and Trilinear Method, revealed an oddity with the Trilinear Method. This specimen was lightly prestressed, and barely satisfied Selection Criterion 4. For this specimen, use of Equation 2-7 to compute I''_{cr}, the transitional stiffness between the uncracked and "fully cracked" I values in the Trilinear Method (i.e., the second slope in Figure 2-4), results in a moment of inertia *less* than the fully cracked I_{cr}, (i.e., the third slope in Figure 2-4). In other words, the equation predicts an effective I value less than the theoretical lower-bound I_{cr} (which is based on a fully cracked section with zero prestress force). This is an illogical result that warrants further investigation. This oddity occurs when the Trilinear Method shift moment M'' (discussed in Section 2.3.3) is controlled by the upper limit of Class T behavior instead of the value computed as 1.5 multiplied by the (zero-curvature) prestress moment, M_0. This occurs when the Class T upper limit is greater than $1.5M_0$, which is more likely in lightly prestressed members.

The Rational Method also greatly overpredicts the post-cracking deflections for Test 101, though not as much as the Trilinear Method. In the Rational Method, the effective moment of inertia, I^*_e, computed in accordance with Equation 2-3, only slightly exceeds the fully cracked I value for this lightly prestressed member.

Some poor predictions that fall within 1.5 times the interquartile range such as beams with reference numbers 30, 31, 33, 71, and 79, have deflections that are so small and imprecisely measured that the percent differences between a predicted value and measured value can appear extreme.

Figure 4-7 shows three other groupings of the results: Class T beams at their maximum service-level stress, Class C beams at their maximum service-level stress, and all beams (combined) at their maximum service-level stress.

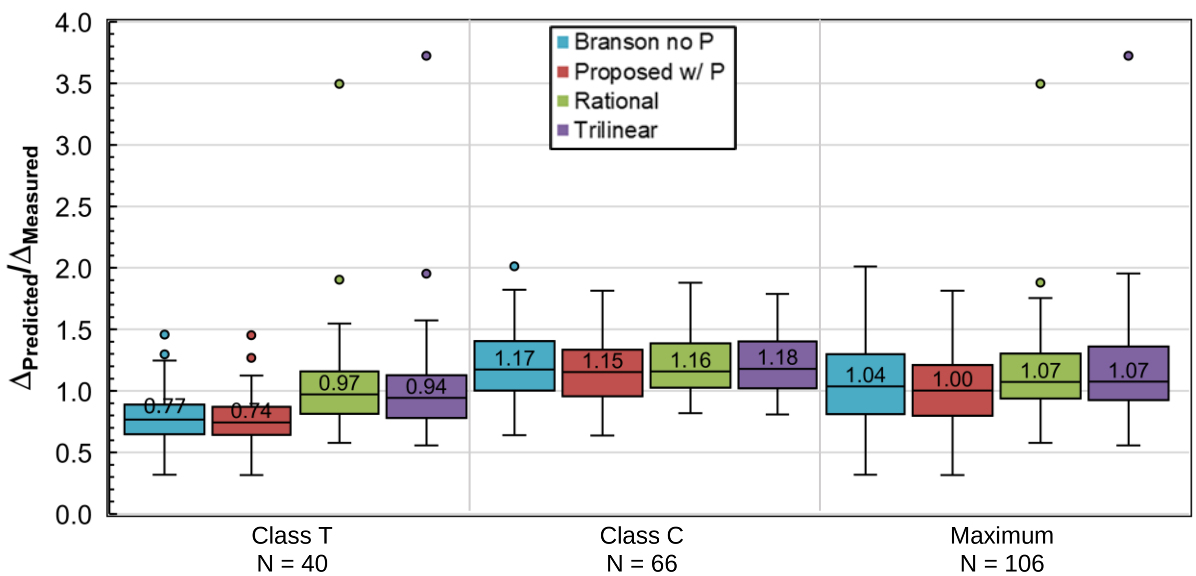

Figure 4-7: Distribution of prediction accuracy for Class T beams, Class C beams, and all beams at the maximum reasonable service load

When subdividing the results into Class T and Class C members at the maximum reasonable service loads, a difference in prediction performance appears. The methods underpredict deflection for Class T members on average. The Rational and Trilinear Methods are slightly more accurate on average but have the same two extreme overprediction values as previously discussed. The Class C prediction performance at the maximum reasonable service load is relatively similar for all four methods and conservative on average, with slightly less dispersion for the Trilinear Method.

One reason for the different performance with respect to the (slightly cracked) Class T beams may be related to the predictability of the *uncracked* portion of the response of the test beams. In order to further evaluate the prediction accuracy for the uncracked portion of the response for the database tests, Figure 4-8, Figure 4-9, and Figure 4-10 illustrate the accuracy and dispersion of the predictions at the $7.5\sqrt{f'_c}$ stress level for yet-to-be-cracked beams. As these predictions are based solely on uncracked-section analysis, they are independent of the four methods evaluated. Note that the prediction of uncracked deflections is worse for the Class T flexural members than for the Class C flexural members in this study. This could contribute to the relative inaccuracy of the post-cracked deflection of these Class T beams.

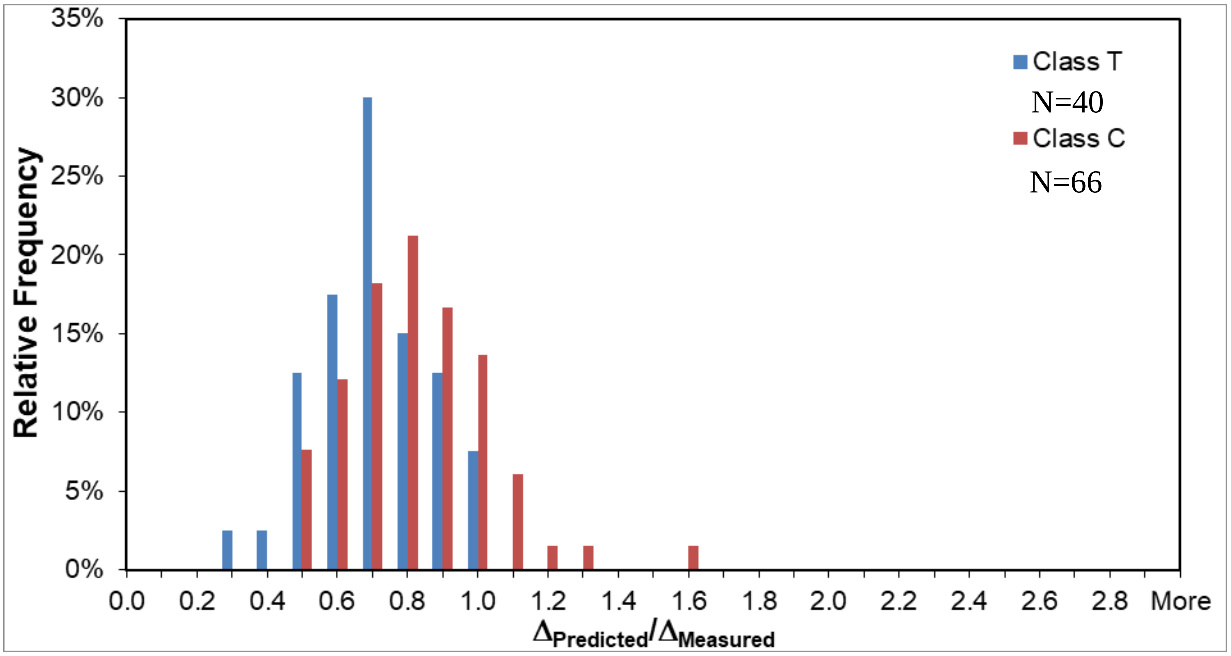

Figure 4-8: Histogram of prediction accuracy by member class at $7.5\sqrt{f'_c}$ stress level.

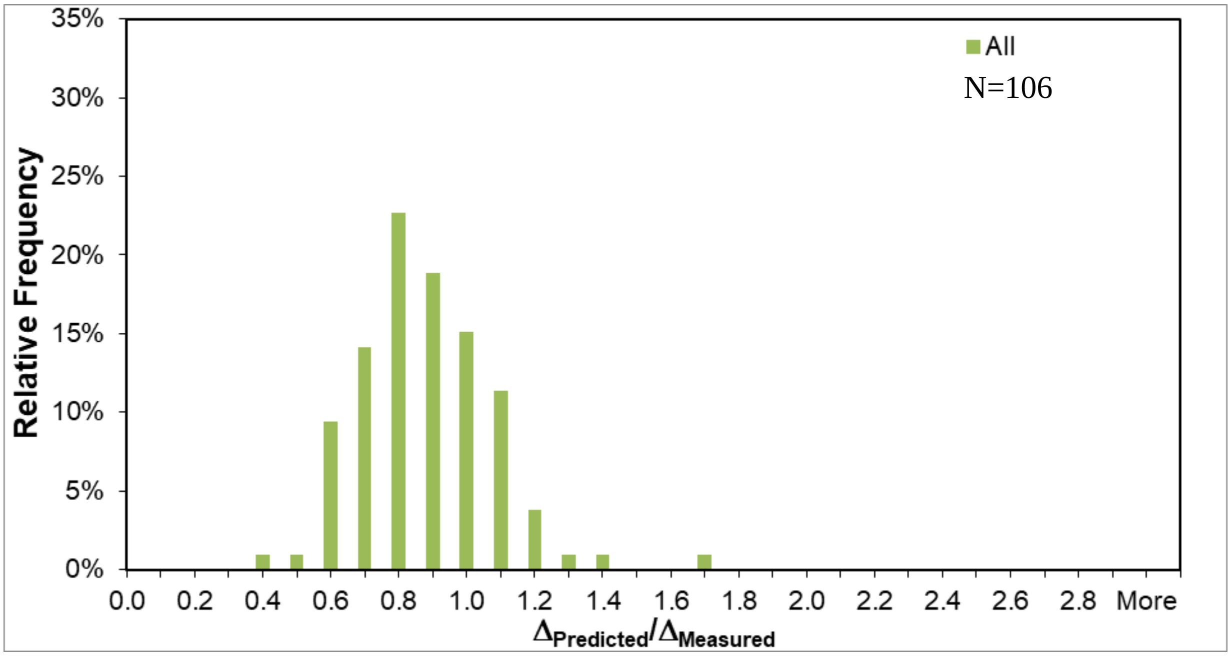

Figure 4-9: Histogram of prediction accuracy for all tests at $7.5\sqrt{f'_c}$ stress level.

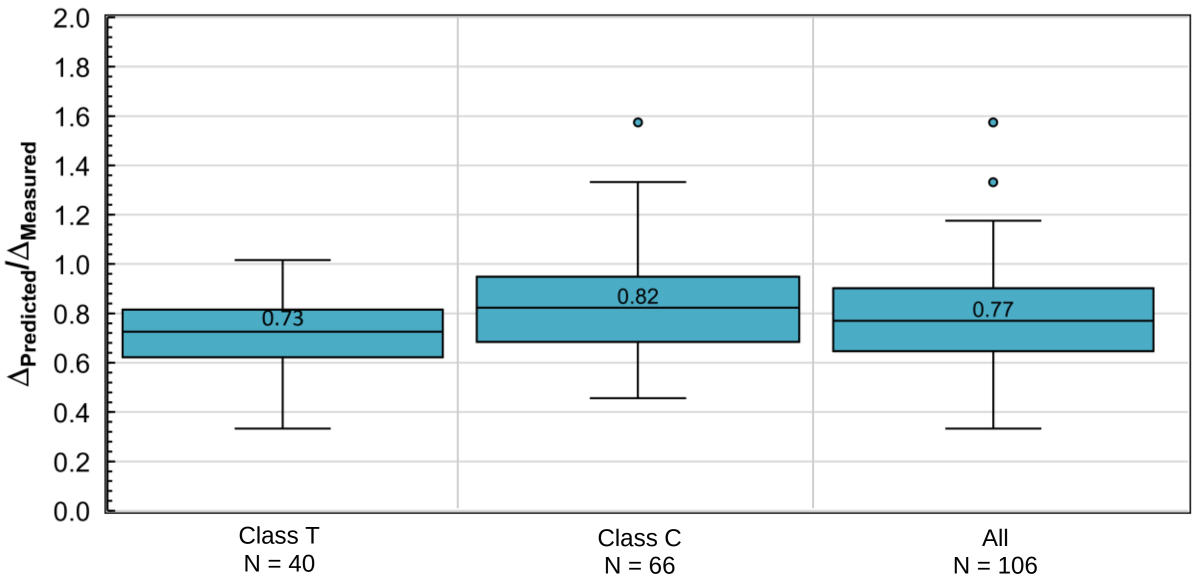

Figure 4-10: Distribution of prediction accuracy for Class T beams, Class C beams, and all beams at $7.5\sqrt{f'_c}$ stress level.

CHAPTER 5: RESEARCH CONCLUSIONS AND RECOMMENDATIONS

5.1 SUMMARY OF WORK

A standard, simple calculation procedure for immediate service-load deflection of a simply supported Class T or Class C prestressed concrete flexural member has not yet been well defined. A database of test results from these types of beams was compiled. Beams were compiled from nine different sources with a total of 106 beams satisfying the selection criteria. Key service load levels and corresponding deflections were determined and recorded from the literature for each test specimen. Four methods of predicting the immediate deflection in prestressed concrete beams were compared including the author's Proposed Method to look at the conservatism and accuracy of each method comparatively to one another.

5.2 CONCLUSIONS

The research presented in this paper supports the following conclusions:

- Including the influence of the prestressing force when calculating I_{cr} results in more accurate predictions on average.
- Both the Rational and Trilinear Methods tend to overpredict beam deflections on average—particularly for lightly prestressed members.
- The Trilinear Method produces an I_e less than I_{cr} in some cases. This is more likely to occur in lightly prestressed members than fully prestressed members.
- Despite its logical complexity, the Rational Method does not yield an improvement in accuracy when compared to the full database of Class T and Class C members.

- The Proposed Method, which features a reasonably simple approach to calculation, produced the most accurate predictions on average with the least amount of dispersion.

5.3 RECOMMENDATIONS FOR FUTURE RESEARCH

Based on the research presented in this thesis, the following recommendations are given for potential future research:

1. Re-evaluate the accuracy of each method after filtering out (or accounting for) the specimens for which uncracked deflections are poorly predicted.
2. Investigate the accuracy of the Trilinear Method if either the partially cracked or fully cracked I_{cr} value is enforced as a lower bound on the effective moment of inertia.
3. Evaluate the accuracy of the methods through means of a well-designed experimental program that incorporates a range of key, well-controlled variables, which would include a range of prestressing levels, combinations of prestressed and nonprestressed reinforcement, concrete modulus of elasticity, concrete tensile strength, common types of cross sections, and loading configurations.

REFERENCES

ACI Committee 423. 1999. “State-of-the-Art Report on Partially Prestressed Concrete (ACI 423.5R-99).” American Concrete Institute, Farmington Hills, MI.

ACI Committee 318. 2019. “Building Code Requirements for Structural Concrete (ACI 318-19) and Commentary (ACI 318R-19).” American Concrete Institute, Farmington Hills, MI.

ACI Committee 318. 2002. “Building Code Requirements for Structural Concrete (ACI 318-02) and Commentary (ACI 318R-02).” American Concrete Institute, Farmington Hills, MI.

Aswad, A., Burnley, G., Cleland, N., Orndorff, D., and Wynings, C. 2004. “Load Testing of Prestressed Concrete Double Tees without Web Reinforcement.” *PCI Journal* V. 49 (2): 66-77.

Bachmann, H. 1984. “Design of Partially Prestressed Concrete Structures Based on Swiss Experiences.” *PCI Journal* V. 29 (4): 84-105.

Bischoff, P. 2005. “Reevaluation of Deflection Prediction for Concrete Beams Reinforced with Steel and Fiber Reinforced Polymer Bars.” *Journal of Structural Engineering* V. 131 (5): 752-767.

Bischoff, P. 2007. “Rational Model for Calculating Deflection of Reinforced Concrete Beams and Slabs.” *Canadian Journal of Civil Engineering* V. 34 (8): 992-1002.

Bischoff, P., and Scanlon, A. 2007. “Effective Moment of Inertia for Calculating Deflections of Concrete Members Containing Steel Reinforcement and FRP Reinforcement.” *ACI Structural Journal* V. 104 (1): 68-75.

Bischoff, P., Naito, C., and Ingaglio, J. 2018. “Immediate Deflection of Partially Prestressed Concrete Flexural Members.” *ACI Structural Journal* V. 115 (6): 1683-1693

Boczkaj, B. 1994. “Section Partially Prestressed — An Exact Solution.” *PCI Journal* V. 39 (6): 99-106.

Branson, D. 1963. “Instantaneous and Time-Dependent Deflections of Simple and Continuous Reinforced Concrete Beams.” HPR Report No. 7, Part 1, Alabama Highway Department, Bureau of Public Roads, Montgomery, AL. 78 pp.

Branson, D. 1977. *Deformation of Concrete Structures*. McGraw-Hill, New York. 546 pp.

Branson, D. 1983. Discussion of “Expedient Service Load Analysis of Cracked Prestressed Concrete Sections.” *PCI Journal* V. 28 (6): 140-141.

Brewe, J., and Myers, J. 2011. “High-Strength Self-Consolidating Concrete Girders Subjected to Elevated Compressive Fiber Stresses, Part II: Structural Behavior.” *PCI Journal* V. 56 (1): 92-109.

Chen, J. 1973. “Integrated Procedures for Predicting the Initial and Time-Dependent Deformation of “Reinforced” Concrete Structures.” Ph.D. Thesis, University of Iowa.

Hernandez, G. 1958. “Strength of Prestressed Concrete Beams with Web Reinforcement.” Ph.D. Thesis, University of Illinois. Issued as a part of the Seventh Progress Report of the Investigation of Prestressed Concrete for Highway Bridges, Civil Engineering Studies, Structural Research Series No. 153.

Janney, J., Hognestad, E., and McHenry, D. 1956. “Ultimate Flexural Strength of Prestressed and Conventionally Reinforced Concrete Beams.” *ACI Structural Journal* V. 27 (6): 601-620.

Mast, R. 1998. “Analysis of Cracked Prestressed Concrete Sections: A Practical Approach.” *PCI Journal* V. 43(4): 80-91

Moustafa, S. 1977. “Design of Partially Prestressed Concrete Flexural Members.” *PCI Journal* V. 22 (3): 13-29

Naaman, A. 1985. “Partially Prestressed Concrete: Review and Recommendations.” *PCI Journal* V. 30 (6): 30-71

Naito, C., Cetisli, F., and Tate, T. 2015. “A Method for Quality Assurance of Seven-Wire Strand Bond in Portland Cement Concrete.” *PCI Journal* V. 60 (4): 69-84.

Nilson, A. 1976. “Flexural Stresses After Cracking in Partially Prestressed Beams.” *PCI Journal* V. 21 (4): 72-81

PCI. 2017. “PCI Design Handbook: Precast and Prestressed Concrete.” Eighth edition, Precast/Prestressed Concrete Institute (PCI), Chicago, IL.

Peterman, R. J. 2009. “A Simple Quality Assurance Test for Strand Bond.” *PCI Journal* V. 54 (2): 143-161.

Saqan, E., and Frosch, R. 2009. “Influence of Flexural Reinforcement on Shear Strength of Prestressed Concrete Beams.” *ACI Structural Journal* V. 106 (1): 60-68.

Shaikh, A. 1967. “Use of Non-Tensioned Steel in Prestressed Concrete Beams.” Ph.D. Thesis, University of Iowa.

Shaikh, A., and Branson, D. 1970. “Non-Tensioned Steel in Prestressed Concrete Beams.” *PCI Journal* V. 15 (1): 14-36.

Sozen, M. 1957. “Strength in Shear of Prestressed Concrete Beams without Web Reinforcement.” Ph.D. Thesis, University of Illinois. Issued as a part of the Sixth Progress Report of the Investigation of Prestressed Concrete for Highway Bridges, Civil Engineering Studies, Structural Research Series No. 139.

Warwaruk, J. 1960. “Strength and Behavior in Flexure of Prestressed Concrete Beams.” Ph.D. Thesis, University of Illinois.

APPENDIX A: NOTATION

a	distance from center of support to nearest concentrated load, in.
A_{cr}	area of concrete section computed for cracked section, in.^{2}
A_g	gross area of concrete section, in.^{2}
A_p	area of prestressed longitudinal tension reinforcement, in.^{2}
A_{ps}	area of prestressed longitudinal tension reinforcement, in.^{2}
A_s	area of nonprestressed longitudinal tension reinforcement, in.^{2}
A'_s	area of nonprestressed longitudinal compression reinforcement, in.^{2}
b_f	width of compression face of member, in.
b_w	web width, in.
c_{cr}	neutral axis (zero stress) depth for cracked section, in.
d_p	distance from extreme compression fiber to centroid of prestressing reinforcement, in.
d_s	distance from extreme compression fiber to centroid of nonprestressed tension reinforcement, in.
d'_s	distance from extreme compression fiber to centroid of nonprestressed compression reinforcement, in.
e	eccentricity of reinforcement relative to centroid of concrete cross section, in.
E_c	modulus of elasticity of concrete at time of testing, ksi
e_{cr}	eccentricity of reinforcement relative to cracked centroid of concrete cross section (cracked section properties do not include effects of prestressing), in.
e'_{cr}	eccentricity of reinforcement relative to cracked centroid of concrete cross section (cracked section properties include effects of prestressing), in.
E_p	elastic modulus of prestressed reinforcement, ksi
$e_{p,cr}$	eccentricity of reinforcement relative to cracked centroid of concrete cross section (cracked section properties include effects of prestressing), in.
f_{bot}	strength of nonprestressed reinforcement at the bottom fiber of member, psi
$f_{bot,D+L}$	strength of nonprestressed reinforcement at the bottom fiber of member under total service load, psi
f'_c	concrete compressive strength, psi
$f'_{c,test}$	concrete compressive strength at time of testing, psi
f_{dc}	tensile strength of prestressing reinforcement at decompression, ksi
f_{pe}	concrete precompression stress at the bottom fiber due to effects of prestressing, psi
$f_{pe,w}$	effective stress in prestressing reinforcement, including effect of self-weight moment, at time of test, ksi
f_{pj}	initial jacking tensile strength of prestressing reinforcement, ksi
f_{ps}	stress in prestressing reinforcement at nominal flexural strength, ksi
f_{pu}	specified tensile strength of prestressing reinforcement, ksi
f_r	concrete modulus of rupture, psi
$f_{r,reported}$	reported modulus of rupture of concrete, psi

f_{se}	effective strength of prestressing reinforcement at time of test under self-weight moment, ksi
f_y	specified yield strength of nonprestressed reinforcement, ksi
h	overall height of member, in.
h_f	flange thickness of member, in.
I''_{cr}	effective moment of inertia used in Trilinear Method from initial cracked moment to calculated shifted moment, in.^{4}
I^*_e	effective moment of inertia used in Rational Method if calculated shift moment is less than the cracked moment, in.^{4}
I_{cr}	moment of inertia of concrete section about cracked centroidal axis (may or may not include effects of prestressing), in.^{4}
I'_{cr}	moment of inertia of concrete section about cracked centroidal axis (includes effects of prestressing), in.^{4}
I_e	effective moment of inertia, in.^{4}
I_g	moment of inertia of gross concrete section about centroidal axis, in.^{4}
I_{tr}	moment of inertia of concrete section about transformed centroidal axis, in.^{4}
I_{ucr}	moment of inertia of gross concrete section about centroidal axis, in.^{4}
K	effective length factor
L	clear span, ft.
L_s	length of nonprestressed longitudinal tension reinforcement, ft.
L_{Total}	full length of member, ft.
M''	moment intercept at second change in slope used in Trilinear Method, kip-in
M_0	moment intercept at for fully cracked section, kip-in
M'_0	moment intercept at for partially cracked section, kip-in
M_1	shifted moment intercept used in Rational Method, kip-in
M'_1	modified shifted moment intercept used in Rational Method if shifted intercept is less than the cracking moment, kip-in
M_a	applied moment intercept, kip-in
M_{cr}	cracking moment intercept, kip-in
M_{D+L}	total service moment intercept, kip-in
M_{dec}	moment causing zero stress at the extreme fiber in the precompressed tension zone, kip-in
M_{dec}	decompression moment applied to prestressed section that corresponds to zero stress at tension face, kip-in
M_F	moment applied to prestressed section when failure occurred in test, kip-in
M_n	nominal flexural strength at section, kip-in
$M_{s.max}$	maximum reasonable service-level moment, kip-in
M_{SD}	superimposed dead load moment intercept, kip-in
M_{self}	self-weight moment intercept, kip-in
$M_{service}$	total service moment intercept, kip-in
M_{shift}	moment intercept taken as the shifted moment in Rational Method, kip-in

M_{SL}	superimposed live load moment intercept, kip-in
$M_{TOTAL,0.6}$	total moment corresponding to a compressive stress of 0.6(fc') at extreme fiber in the compression zone, kip-in
$M_{TOTAL,10}$	total moment corresponding to a tensile stress of $10\sqrt{fc'}$ at extreme fiber in the precompressed tension zone, kip-in
$M_{TOTAL,12}$	total moment corresponding to a tensile stress of $12\sqrt{fc'}$ at extreme fiber in the precompressed tension zone, kip-in
$M_{TOTAL,6}$	total moment corresponding to a tensile stress of $6\sqrt{fc'}$ at extreme fiber in the precompressed tension zone, kip-in
$M_{TOTAL,7.5}$	total moment corresponding to a tensile stress of $7.5\sqrt{fc'}$ at extreme fiber in the precompressed tension zone, kip-in
M_V	total moment corresponding to observation of shear crack initiation in test, kip-in
M_w	self-weight moment, kip-in
M_{zc}	zero-curvature moment intercept, kip-in
n_p	modular ratio
NR	Not Reported
Ø	nominal diameter of reinforcement, in.
P	applied prestress force, kip
P_0	effective force of prestressing reinforcement at decompression, kip
P_e	effective force of prestressing reinforcement at time of test under self-weight moment after losses, kip
$P_{failure}$	load at which member failed, kip
PL	Point Load
Rect.	Rectangular section
S_b	section modulus for tension face, in.^{3}
S_t	section modulus for compression face, in.^{3}
Tee	Tee Shape
TT	Double-tee Shape
w'_1	load that is associated with the shifted moment (M_{shift}) at the critical cracking location, lb/ft
w_{cr}	load that is associated with the cracking moment (M_{cr}) at the critical cracking location, lb/ft
w_D	dead load, lb/ft
w_{D+L}	total service load, lb/ft
w_{dec}	decompression load that corresponds to zero stress at tension face, lb/ft
w_{SD}	superimposed dead load, lb/ft
w_{self}	self-weight load, lb/ft
w_{shift}	load that is associated with the shifted moment (M'') at the critical cracking location, lb/ft
w_{SL}	superimposed live load, lb/ft
y_b	distance from centroid to extreme fiber of precompressed tension zone (bottom), in.
$\bar{y}'_{cr}$	distance from cracked section centroid to extreme compression fiber (top), in.

y_t	distance from centroid to extreme compression fiber (top), in.
$y_{t,gross}$	distance from centroid of gross section to extreme compression (top) fiber, in.
$y_{top,cr}$	distance from cracked section centroid to extreme compression fiber (top), in.
Δ	deflection, in.
Δ_D	immediate deflection due to dead load, in.
Δ_{D+L}	total immediate deflection, in.
Δ_{dec}	decompression deflection that corresponds to zero stress at tension face, in.
Δ_L	immediate deflection due to live load, in.
$\Delta_{Measured}$	measured deflection, in.
$\Delta_{Predicted}$	predicted deflection, in.
$\Delta_{test,10}$	deflection of member at load corresponding to computed (uncracked) stress of $10\sqrt{fc'}$ at extreme fiber of precompressed tension zone, in.
$\Delta_{test,12}$	deflection of member at load corresponding to computed (uncracked) stress of $12\sqrt{fc'}$ at extreme fiber of precompressed tension zone, in.
$\Delta_{test,6}$	deflection of member at load corresponding to computed (uncracked) stress of $6\sqrt{fc'}$ at extreme fiber of precompressed tension zone, in.
$\Delta_{test,7.5}$	deflection of member at load corresponding to computed (uncracked) stress of $7.5\sqrt{fc'}$ at extreme fiber of precompressed tension zone, in.
$\Delta_{test,max}$	deflection of member at load corresponding to computed maximum reasonable service level moment, in.
ρ_p	reinforcement ratio

APPENDIX B: CALCULATION EXAMPLES

Given information from example 5.2.2.3 (8th Ed. PCI Handbook)

10' wide, 24" deep double-tee (10DT24) with a single drape point at midspan as shown in Figure A-1.

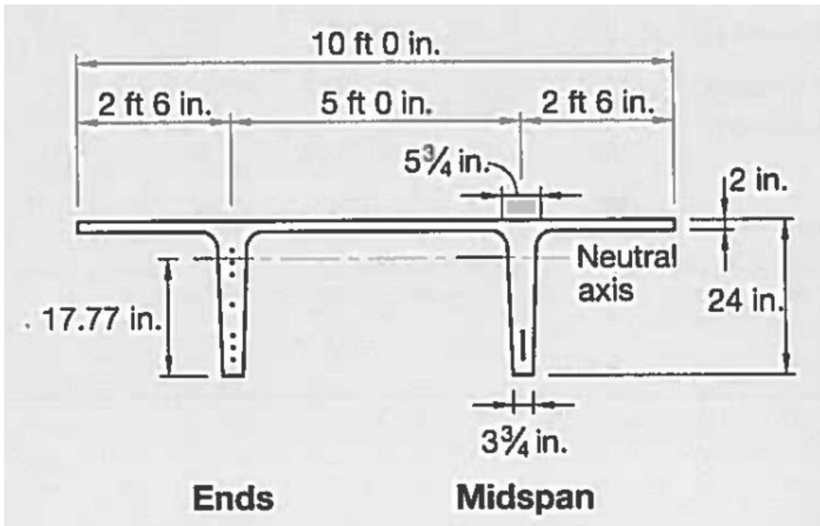

Figure A-1: 10DT24 from PCI Design Handbook

$L = 70$ ft

$h = 24$ in.

$h_f = 2$ in.

$b_f = 120$ in.

$b_w = 9.5$ in. (Assumed average width of the two stems combined)

Concrete

$f'_c = 5{,}000$ psi, normal weight

$E_c = 4287$ ksi

Prestressing steel

$A_{ps} = 2.142$ in.^{2}

Fourteen ½ in. diameter, grade 270, low-relaxation, seven-wire strands

Section properties (gross)

$A_g = 449$ in.^{2}

$I_g = 22469$ in.^{4}

$y_b = 17.77$ in.

$y_t = 6.23$ in.

$S_b = 1264$ in.^{3}

$S_t = 3607$ in.^{3}

Eccentricities and depth of prestressing

$e = 4.91$ in. @ ends

$e = 14.27$ in. @ midspan

$e = 12.40$ in. @ 0.4L (assumed critical cracking location for single-point draping)

$d_p = e + y_t = 12.40 + 6.23 = 18.63$ in. @ 0.4L (critical location for cracking)

Prestress force

$E_p = 28{,}500$ ksi

$f_{pu} = 270$ ksi

$f_{pj} = 0.75 f_{pu} = 0.75(270) = 202.5$ ksi

Effective prestress stress = $f_{se} = 0.8 f_{pj} = 0.8(202.5) = 162$ ksi (assuming 20% total losses and effective prestress under self-weight)

Loads

Self-weight = $w_{self} = 468$ lb/ft

Superimposed dead load = $w_{SD} = 100$ lb/ft

Total dead load = $w_D = w_{self} + w_{SD} = 468 + 100 = 568$ lb/ft

Live load (superimposed) = $w_{SL} = 300$ lb/ft

Total service load = $w_{D+L} = w_{self} + w_{SD} + w_{SL} = 468 + 100 + 300 = 868$ lb/ft

Bending moments

$M_{service} = M_{D+L} = \frac{(w_{D+L})(l^2)}{8} = \frac{(0.868)(70)^2(12)}{8} = 6380$ kip-in. @ midspan

Because the beam has a single drape point, it is most susceptible to cracking at or near 0.4L along the span.

$M_{service} = M_{D+L} = 0.96(6380) = 6125$ kip-in. @ 0.4L (critical location for cracking)

Load	Midspan Section	0.4L Section
w_{self}	3440 kip-in	3302 kip-in
w_{SD}	735 kip-in	706 kip-in
w_{SL}	2205 kip-in	2117 kip-in

Determine beam classification and compute deflection due to dead load

Check cracking conditions at 0.4L (using gross-section analysis for simplicity).

$$f_{bot} = -\frac{P}{A} - \frac{Pe}{S_b} + \frac{M}{S_b}$$

$P_e = A_{ps} f_{se} = 2.142(162) = 347$ kips (effective prestress force after losses)

$\frac{P_e}{A} = \frac{347}{449} = 773$ psi (compression)

$\frac{P_e e}{S_b} = \frac{347(12.4)}{1264} = 3404$ psi (compression)

$\frac{M_{self}}{S_b} = \frac{3302}{1264} = 2613$ psi (tension)

$\frac{M_{SD}}{S_b} = \frac{706}{1264} = 558$ psi (tension)

$\frac{M_{SL}}{S_b} = \frac{2117}{1264} = 1675$ psi (tension)

Cracking stress, $f_r = 7.5\lambda\sqrt{f'_c} = 7.5(1.0)\sqrt{5000} = 530$ psi (tension)

f_{bot} due only to prestressing = $-773 - 3404 = -4177$ psi (compression)

f_{pe} = 4177 psi, concrete precompression stress at the bottom fiber due to effects of prestressing (compression positive in ACI 318)

Cracking stress, $f_r = 7.5\lambda\sqrt{f'_c} = 7.5(1.0)\sqrt{5000} = 530$ psi (tension)

f_{bot} under dead load = $-4177 + 2612 + 559 = -1006$ psi (compression)

The double-tee is UNCRACKED under dead load (w_D)

f_{bot} under service load = $-4177 + 2613 + 558 + 1675 = 669$ psi (tension)

The double-tee is CRACKED under service load (w_{D+L})

$f_{bot,D+L} = 669$ psi $= 9.5\sqrt{f'_c}$ → This is a CLASS T beam

Dead load deflection (Δ_D) calculation (for all methods) due to beam being uncracked under total dead load (w_D)

$$\Delta = \frac{5wL^4}{384(E_c)I} = \frac{5(70\cdot 12)^4}{384(4287000)}\left(\frac{w}{I}\right) = 1512.2\ \frac{in^4}{psi}\left(\frac{w}{I}\right)$$

$$\Delta_D = 1512.2\left(\frac{w_D}{I_g}\right) = 1512.2\left[\frac{568\left(\frac{1}{12}\right)}{22469}\right] = 3.19 \text{ in. @ midspan}$$

Proposed Method for service load deflections

For the portion of Δ up to decompression (M_{dec}) at the critical cracking location, use

$$\Delta_{dec}= \frac{5wL^4}{384(E_c)I} = 1512.2\left(\frac{w_{dec}}{I_g}\right)$$

Where w_{dec} is the load that causes decompression (M_{dec}) at the critical cracking location (0.4L).

And for the portion of Δ from decompression to full service load, use

$$\Delta= \frac{5wL^4}{384(E_c)I} = 1512.2\left(\frac{w_{D+L} - w_{dec}}{I_e}\right)$$

Where I_e is the effective moment of inertia including the effects of cracking and the prestress force at the critical cracking location (0.4L).

Decompression load ($\boldsymbol{w_{dec}}$) and deflection ($\boldsymbol{\Delta_{dec}}$) calculation

Find w_{dec}:

Stress at bottom fiber = $f_{bot} = 0 = -\frac{P}{A} - \frac{Pe}{S_b} + \frac{M_{dec}}{S_b}$ @ 0.4L

Decompression Moment = $M_{dec} = S_b\left(\frac{P}{A} + \frac{Pe}{S_b}\right) = S_b f_{pe} = 1264(4177) = 5280$ kip-in.

$M_{dec} = 0.96\left(\frac{w_{dec}(L^2)}{8}\right)$ at the 0.4L cross section

$w_{dec} = \frac{8M_{dec}}{0.96L^2} = \frac{8(5280)(\frac{1}{12})}{0.96(70)^2} = 748$ lb/ft

$\Delta_{dec}= 1512.2\left(\frac{w_{dec}}{I_g}\right) = 1512.2\left[\frac{748(\frac{1}{12})}{22469}\right] = 4.20$ in. (total deflection up to decompression load, w_{dec})

Calculation of portion of deflection between decompression and full service load

Calculate I_{cr}:

Cracked-section properties at $M = M_{D+L} = 6125$ kip-in at 0.4L cross section computed using Mast's (1998) iterative approach including the effect of prestress force.

$c_{cr} = 15.51$ in. (neutral axis [zero stress] depth)

$y_{top,cr} = 4.26$ in. (centroid depth)

$e_{p,cr} = 14.37$ in. (eccentricity)

$A_{cr} = 383$ in.^{2}

$I_{cr} = 10117$ in.^{4} (about the centroid of the cracked section)

Determine cracking moment

$S_b = 1264$ in.^{3}

$f_r = 530$ psi

$M_{cr} = S_b(f_r + f_{pe}) = 1264(530 + 4177) = 5950$ kip-in. @ 0.4L (critical location for cracking)

Calculate I_e (for portion of Δ between M_{dec} and $M_a = M_{D+L}$)

$$I_e = \left(\frac{M_{cr} - M_{dec}}{M_a - M_{dec}}\right)^3 \times I_g + \left[1 - \left(\frac{M_{cr} - M_{dec}}{M_a - M_{dec}}\right)^3\right] \times I_{cr}$$

$$I_e = \left(\frac{5950 - 5280}{6125 - 5280}\right)^3 \times 22469 + \left[1 - \left(\frac{5950 - 5280}{6125 - 5280}\right)^3\right] \times 10117$$

$$I_e = \left(\frac{670}{845}\right)^3 \times 22469 + \left[1 - \left(\frac{670}{845}\right)^3\right] \times 10117$$

$I_e = 11222 + 5064 = 16286$ in.^{4}

Calculate total service load deflection (Δ_{D+L})

$$\Delta_{D+L} = \Delta_{dec} + 1512.2\left(\frac{w_{D+L} - w_{dec}}{I_e}\right)$$

$$\Delta_{D+L} = 4.20 + 1512.2\left(\frac{(868-748)\left(\frac{1}{12}\right)}{16286}\right) = 4.20 + 0.93 = 5.13 \text{ in.}$$

Calculate immediate deflection due to live load (Δ_L)

$$\Delta_L = \Delta_{D+L} - \Delta_D = 5.13 - 3.19$$

$$\boxed{\Delta_L = 1.94\ \text{in.} = L/434}$$

Branson No Precompression Method Example

For the portion of Δ up to decompression at the critical cracking location (0.4L), use

$$\Delta_{dec} = \frac{5wL^4}{384(E_c)I} = 1512.2\left(\frac{w_{dec}}{I_g}\right)$$

Where w_{dec} is the load that causes decompression (M_{dec}) at the critical cracking location.

And for the portion of Δ from decompression to full service load, use

$$\Delta = \frac{5wL^4}{384(E_c)I} = 1512.2\left(\frac{w_{D+L} - w_{dec}}{I_e}\right)$$

Where I_e is the effective moment of inertia including the effects of cracking but computed using a "fully cracked" I_{cr} that does not include the effect of the prestress force.

Decompression load and deflection calculation

Find w_{dec}:

Stress at bottom fiber = $f_{bot} = 0 = -\frac{P}{A} - \frac{P(e)}{S_b} + \frac{M_{dec}}{S_b}$ @ 0.4L

Decompression Moment = $M_{dec} = S_b f_{pe} = 1264(4177) = 5280$ kip-in.

$M_{dec} = 0.96\left(\frac{w_{dec}(l^2)}{8}\right)$ at the 0.4L cross section

$w_{dec} = \frac{8M_{dec}}{0.96L^2} = \frac{8(5280)(\frac{1}{12})}{0.96(70)^2} = 748$ lb/ft

$\Delta_{dec} = 1512.2\left(\frac{w_{dec}}{I_g}\right) = 1512.2\left[\frac{748\left(\frac{1}{12}\right)}{22469}\right] = 4.20$ in. (total deflection up to decompression load, w_{dec})

Calculation of portion of deflection between decompression and full service load.

Calculate "fully cracked" I_{cr}

This "fully cracked" I_{cr} computation is the same procedure used in the PCI Handbook (8th ed.). It assumes zero prestress force and a uniform-width cross section (i.e., the neutral axis is in the flange of this double tee).

$A_{ps} = 2.142$ in.^{2}

$b_f = 120$ in.

$d_p = e + y_t = 12.40 + 6.23 = 18.63$ in. @ 0.4L (critical location for cracking)

$$\rho_p = \frac{A_{ps}}{bd_p} = \frac{2.142}{120(18.63)} = 0.000958$$

$$n_p = \frac{E_p}{E_c} = \frac{28500}{4287} = 6.65$$

$$I_{cr} \approx n_p A_{ps}\left(d_p\right)^2\left(1 - 1.6\sqrt{n_p \rho_p}\right)$$

$I_{cr} = 6.65(2.142)(18.63)^2\left(1 - 1.6\sqrt{6.65 \times 0.000958}\right) = 4310$ in^4

Determine cracking moment

$S_b = 1264$ in.^{3}

$f_r = 530$ psi

$f_{pe} = 4177$ psi

$M_{cr} = S_b\left(f_r + f_{pe}\right) = 1264(530 + 4177) = 5950$ kip-in. @ 0.4L (critical location for cracking)

Calculate I_e

$$I_e = \left(\frac{M_{cr} - M_{dc}}{M_a - M_{dc}}\right)^3 I_g + \left[1 - \left(\frac{M_{cr} - M_{dc}}{M_a - M_{dc}}\right)^3\right] I_{cr}$$

$$I_e = \left(\frac{5950 - 5280}{6125 - 5280}\right)^3 \times 22469 + \left[1 - \left(\frac{5950 - 5280}{6125 - 5280}\right)^3\right] \times 4310$$

$$I_e = \left(\frac{670}{845}\right)^3 \times 22469 + \left[1 - \left(\frac{670}{845}\right)^3\right] \times 4310$$

$$I_e = 11222 + 2160 = 13380 \text{ in.}^4$$

Calculate service deflection

$$\Delta_{D+L} = \Delta_{dec} + 1512.2\left(\frac{w_{D+L} - w_{dec}}{I_e}\right)$$

$$\Delta_{D+L} = 4.20 + 1512.2\left(\frac{(868-748)\left(\frac{1}{12}\right)}{13380}\right) = 4.20 + 1.13 = 5.33 \text{ in.}$$

Calculate immediate deflection due to live load

$$\Delta_L = \Delta_{D+L} - \Delta_D = 5.33 - 3.19$$

$$\boxed{\Delta_L = 2.14 \text{ in.} = L/393}$$

Rational Method Example

Determine cracking moment

$S_b = 1264$ in.^{3}

$f_r = 530$ psi

$f_{pe} = 4177$ psi

$M_{cr} = S_b(f_r + f_{pe}) = 1264(530 + 4177) = 5950$ kip-in. @ 0.4L (critical location for cracking)

$M_a = M_{service} = M_{D+L} = 6125$ kip-in. @ 0.4L (critical location for cracking)

$M_a > M_{cr}$

Compute decompression force

Assuming given effective prestress, f_{se}, occurs simultaneously with the self-weight moment at the critical cracking location

$f_{se} = 162$ ksi

$P_e = 347$ kips (effective prestress force after losses)

$$f_{dc} = f_{se} + n_p\left(\frac{P_e}{A_g} + \frac{P_e e_p^2}{I_g}\right) - n_p\left(\frac{M_{self}\,e_p}{I_g}\right)$$

Where M is equal to the self-weight moment (M_{self}) at the critical cracking location.

$$n_p = \frac{E_p}{E_c} = \frac{28500}{4287} = 6.65$$

$$f_{dc} = 162 + 6.65\left(\frac{347}{449} + \frac{347(12.4)^2}{22469}\right) - 6.65\left(\frac{3302(12.4)}{22469}\right)$$

$f_{dc} = 170.8$ ksi

$P_0 = f_{dc}A_{ps} = 170.8(2.142) = 365.9$ kip

Compute "fully cracked" properties @ 0.4L (these properties do not include the effects of prestressing)

$$\rho_p = \frac{A_{ps}}{bd_p} = \frac{2.142}{120(18.63)} = 0.000958$$

$c_{cr} = d_p\left[\sqrt{(n_p\rho_p)^2 + 2n_p\rho_p} - n_p\rho_p\right]$ (assuming neutral axis is in the flange)

$$= 18.63\left[\sqrt{(6.65 \times 0.000958)^2 + 2(6.65)(0.000958)} - 6.65(0.000958)\right]$$

$$= 18.63[0.1067]$$

$c_{cr} = 1.99$ in.

$I_{cr} \approx n_p A_{ps}\left(d_p\right)^2\left(1 - 1.6\sqrt{n_p\rho_p}\right)$ (assuming neutral axis is in the flange)

$I_{cr} = 6.65(2.142)(18.63)^2\left(1 - 1.6\sqrt{6.65 \times 0.000958}\right) = 4310$ in^4

$e_{cr} = d_p - c_{cr} = 18.63 - 1.99 = 16.64$ in.

Compute partially cracked section properties at full service load moment

Cracked-section properties at $M = M_{D+L} = 6125$ kip-in at 0.4L cross section computed using Mast's (1998) iterative approach including the effect of prestress force.

$c'_{cr} = 15.51$ in. neutral axis [zero stress] depth; (c_{cr} in Proposed Method)

$\bar{y}'_{cr} = 4.26$ in. (centroid depth); ($y_{top,cr}$ in Proposed Method)

$e'_{cr} = 14.37$ in. (eccentricity); ($e_{p,cr}$ in Proposed Method)

$A'_{cr} = 383$ in.^{2} ; (A_{cr} in Proposed Method)

$I'_{cr} = 10117$ in.^{4} ; (I_{cr} in Proposed Method)

Find key bending moment values at critical location for cracking

$M_a = M_{D+L} = 6125$ kip-in. @ 0.4L (critical location for cracking)

$M_{zc} = P_0 e_g = 365.9(12.40) = 4537$ kip-in (zero-curvature moment)

$M_o = P_0 e_{cr} = 365.9(16.64) = 6089$ kip-in (moment intercept for fully cracked section)

$M_1 = \frac{\left[M_o - M_{zc}\left(\frac{I_{cr}}{I_g}\right)\right]}{1-\frac{I_{cr}}{I_g}} = \frac{6089-4537\left(\frac{4310}{22469}\right)}{1-\frac{4310}{22469}} = \frac{6089-863}{1-0.1903} = 6450$ kip-in (shifted moment intercept)

$M_{cr} = 5950$ kip-in.

Because $M_1 > M_{cr}$, must modify the shifted moment intercept to M'_1

$$M'_1 = \frac{\left[M'_o - M_{zc}\left(\frac{I'_{cr}}{I_g}\right)\right]}{1-\frac{I'_{cr}}{I_g}}$$

$M'_o = P_0 e'_{cr} = 365.9(14.37) = 5258$ kip-in (moment intercept for partially cracked section)

$M'_1 = \frac{\left[M'_o - M_{zc}\left(\frac{I'_{cr}}{I_g}\right)\right]}{1-\frac{I'_{cr}}{I_g}} = \frac{5258-4537\left(\frac{10117}{22469}\right)}{1-\frac{10117}{22469}} = 5849$ kip-in @ 0.4L

If $\left(M'_1 = M_{shift}\right) < M_{cr}$ then use $I_e^* = \frac{I'_{cr}}{1-\left(\frac{M_{cr}-M'_1}{M_a-M'_1}\right)^2\left(1-\frac{I'_{cr}}{I_g}\right)}$

If $\left(M'_1 = M_{shift}\right) > M_{cr}$ then use $I_e^* = I'_{cr}$

Because $\left(M'_1 = M_{shift}\right) < M_{cr}$,

$$I_e^* = \frac{I'_{cr}}{1-\left(\frac{M_{cr}-M'_1}{M_a-M'_1}\right)^2\left(1-\frac{I'_{cr}}{I_g}\right)} = \frac{10117}{1-\left(\frac{5950-5849}{6125-5849}\right)^2\left(1-\frac{10117}{22469}\right)} = 10920 \text{ in.}^4$$

Calculate service deflection

For the portion of Δ up to the shift moment at the critical cracking location (0.4L), use

$$\Delta = \frac{5wL^4}{384(E_c)I} = 1512.2\left(\frac{w'_1}{I_g}\right)$$

Where w'_1 is the load that is associated with the shifted moment (M_{shift}) at the critical cracking location.

And for the portion of Δ from decompression to full service load, use

$$\Delta = \frac{5wL^4}{384(E_c)I} = 1512.2\left(\frac{w_{D+L} - w_1'}{I_e^*}\right)$$

Where I_e^* is the effective moment of inertia including the effects of cracking and the prestress force.

$$w'_1 = \frac{8M_1'}{0.96L^2} = \frac{8(5849)(\frac{1}{12})}{0.96(70)^2} = 829 \text{ lb/ft}$$

$$\Delta_{D+L} = 1512.2\left(\frac{w_1'}{I_g}\right) + 1512.2\left(\frac{w_{D+L} - w_1'}{I_e^*}\right)$$

$$\Delta_{D+L} = 1512.2\left(\frac{829\left(\frac{1}{12}\right)}{22469}\right) + 1512.2\left(\frac{(868-829)\left(\frac{1}{12}\right)}{10920}\right) = 4.65 + 0.45 = 5.10 \text{ in.}$$

Calculate immediate deflection due to live load

$$\Delta_L = \Delta_{D+L} - \Delta_D = 5.10 - 3.19$$

$$\boxed{\Delta_L = 1.91 \text{ in.} = L/440}$$

Trilinear Method Example

$S_b = 1264$ in.^{3}

$f'_c = 5{,}000$ psi

$f_{pe} = 4177$ psi

Fully Cracked Properties @ 0.4L (see previous methods for calculations)

$c_{cr} = 1.99$ in.

$I_{cr} = 4310$ in^4

$e_{cr} = 16.64$ in.

Decompression force (see Rational Method for calculations)

$f_{dc} = 170.8$ ksi

$P_0 = 365.9$ kip

Moment Intercepts @ 0.4L

$M_{cr} = 5950$ kip-in (see previous methods)

$M_{zc} = 4537$ kip-in (zero-curvature moment; see Rational Method)

$M_o = 6089$ kip-in (moment intercept for fully cracked section; see Rational Method)

$$M" = \text{MAX}\begin{cases} 1.5M_0 = 1.5(6089) = 9134 \text{ kip-in} \\ S_b\left(12\sqrt{f'_c} + f_{pe}\right) = 1264\left(12\sqrt{5000} + 4177\right) = 6352 \text{ kip-in} \end{cases}$$

$M" = 9134$ kip-in (moment at second change in slope)

Calculate Second Slope

$$I"_{cr} = \left[\frac{(M" - M_{cr})}{(M" - M_0) - (M_{cr} - M_{zc})\left(\frac{I_{cr}}{I_g}\right)}\right] I_{cr}$$

$$= \left[\frac{(9134-5950)}{(9134-6089)-(5950-4537)\left(\frac{4310}{22469}\right)}\right] 4310$$

$$= \left[\frac{3184}{(3045)-(1413)\left(\frac{4310}{22469}\right)}\right]4310$$

$I"_{cr} = 4950$ in.^{4}

Calculate Service Deflection

For the portion of Δ up to the cracking moment at the critical cracking location (0.4L), use

$$\Delta = \frac{5wL^4}{384(E_c)I} = 1512.2\left(\frac{w_{cr}}{I_g}\right)$$

Where w_{cr} is the load that is associated with the cracking moment (M_{cr}) at the critical cracking location (0.4L).

$$w_{cr} = \frac{8M_{cr}}{0.96L^2} = \frac{8(5950)(\frac{1}{12})}{0.96(70)^2} = 843 \text{ lb/ft}$$

For the portion of Δ from cracking moment to a shifted moment, use

$$\Delta = \frac{5wL^4}{384(E_c)I} = 1512.2\left(\frac{w_{shift} - w_{cr}}{I"_{cr}}\right)$$

Where w_{shift} is the load that is associated with the shifted moment ($M"$) at the critical cracking location, and

Where $I"_{cr}$ is the effective moment of inertia including the effects of cracking and the prestress force.

$$w_{shift} = \frac{8M"}{0.96L^2} = \frac{8(9134)(\frac{1}{12})}{0.96(70)^2} = 1294 \text{ lb/ft}$$

For the portion of Δ beyond the shifted moment up to the full service load, use

$$\Delta = \frac{5wL^4}{384(E_c)I} = 1512.2\left(\frac{w_{D+L} - w_{shift}}{I_{cr}}\right)$$

$M_{cr} < M_a < M"$ $(5950 < 6125 < 9756)$

For this example, the service-load moment is less than $M"$; therefore, the total deflection is in the second branch (slope). Thus, only two deflection portions are computed:

$$\Delta_{D+L} = 1512.2\left(\frac{w_{cr}}{I_g}\right) + 1512.2\left(\frac{w_{D+L} - w_{cr}}{I"_{cr}}\right)$$

$$\Delta_{D+L} = 1512.2\left(\frac{843\left(\frac{1}{12}\right)}{22469}\right) + 1512.2\left(\frac{(868-843)\left(\frac{1}{12}\right)}{4950}\right) = 4.73 + 0.64 = 5.37 \text{ in.}$$

Calculate Immediate Deflection due to Live Load

$$\Delta_L = \Delta_{D+L} - \Delta_D = 5.37 - 3.19$$

$$\boxed{\Delta_L = 2.18 \text{ in.} = L/385}$$

APPENDIX C: DATABASE OF CLASS T AND CLASS C SIMPLY SUPPORTED PRESTRESSED BEAM TESTS

Table C-1: Specimen Identification, Cross-Sectional Properties, and Concrete Material Properties

Ref #	Reference Author(s)	Beam ID	Cross Section Type	h (in.)	b_f (in.)	h_f (in.)	b_w (in.)	$y_{t,gross}$ (in.)	A_g (in.^{2})	I_g (in.^{4})	$f'_{c,test}$ (psi)	$f_{r,reported}$ (psi)	E_c used (ksi)
1	Naito, Cetisli, Tate	NR-12	Rect	6.0	8.00	6.00	8.00	3.00	48.0	144	9370	NR	**5520**
2	Brewe, Myers	B-84	Tee	12.0	10.00	3.00	4.00	4.77	66.0	855	9000	NR	4600
3	Brewe, Myers	B-75	Tee	12.0	10.50	3.00	4.50	4.88	72.0	935	9000	NR	4600
4	Brewe, Myers	B-68	Tee	12.0	11.00	3.00	5.00	4.96	78.0	1014	9000	NR	4600
5	Aswad et al.	DT-1	TT	30.0	4.00	4.00	12.90	7.20	911	61708	6270	572	4700
6	Aswad et al.	DT-2	TT	30.0	4.00	4.00	10.76	6.67	856	54827	5890	700	4700
7	Aswad et al.	DT-3	TT	30.0	4.00	4.00	14.00	7.63	940	68322	7130	592	4700
8	Saqan, Frosch	V-4-0.93	Rect	28.0	14.50	28.00	14.50	14.00	406	26525	7650	NR	**4990**
9	Saqan, Frosch	V-4-2.37	Rect	28.0	14.68	28.00	14.68	14.00	411	26855	7750	NR	**5020**
10	Saqan, Frosch	V-7-0	Rect	28.0	14.12	28.00	14.12	14.00	395	25830	7900	NR	**5070**
11	Saqan, Frosch	V-7-1.84	Rect	28.0	14.25	28.00	14.25	14.00	399	26068	7700	NR	**5000**
12	Saqan, Frosch	V-7-2.37	Rect	28.0	14.00	28.00	14.00	14.00	392	25611	7700	NR	**5000**
13	Saqan, Frosch	V-10-0	Rect	28.0	14.25	28.00	14.25	14.00	399	26068	7500	NR	**4940**
14	Saqan, Frosch	V-10-1.51	Rect	28.0	14.25	28.00	14.25	14.00	399	26068	7500	NR	**4940**
15	Saqan, Frosch	V-10-2.37	Rect	28.0	14.25	28.00	14.25	14.00	399	26068	7500	NR	**4940**
16	Shaikh	Series I.1	Rect	8.0	6.00	8.00	6.00	4.00	48.0	256	5400	806	**4190**
17	Shaikh	Series I.2	Rect	8.0	6.00	8.00	6.00	4.00	48.0	256	5400	806	**4190**
18	Shaikh	Series I.3	Rect	8.0	6.00	8.00	6.00	4.00	48.0	256	5400	806	**4190**
19	Shaikh	Series II.1	Rect	8.0	6.00	8.00	6.00	4.00	48.0	256	5890	855	**4370**
20	Shaikh	Series II.2	Rect	8.0	6.00	8.00	6.00	4.00	48.0	256	5890	855	**4370**
21	Shaikh	Series II.3	Rect	8.0	6.00	8.00	6.00	4.00	48.0	256	5890	855	**4370**
22	Shaikh	Series III.1	Rect	8.0	6.00	8.00	6.00	4.00	48.0	256	6570	894	**4620**
23	Shaikh	Series III.2	Rect	8.0	6.00	8.00	6.00	4.00	48.0	256	6570	894	**4620**
24	Shaikh	Series III.3	Rect	8.0	6.00	8.00	6.00	4.00	48.0	256	6570	894	**4620**
25	Shaikh	Series IV.1	Rect	8.0	6.00	8.00	6.00	4.00	48.0	256	5880	830	**4370**

NOTES:
E_c used is **Bold** if calculated using the reported $f'_{c,test}$ value. Otherwise, E_c is the value reported in the primary source.

Table C-1: Specimen Identification, Cross-Sectional Properties, and Concrete Material Properties (Cont.)

Ref #	Reference Author(s)	Beam ID	Cross Section Type	h (in.)	b_f (in.)	h_f (in.)	b_w (in.)	$y_{t,gross}$ (in.)	A_g (in.^{2})	I_g (in.^{4})	$f'_{c,test}$ (psi)	$f_{r,reported}$ (psi)	E_c used (ksi)
26	Shaikh	Series IV.2	Rect	8.0	6.00	8.00	6.00	4.00	48.0	256	5880	830	**4370**
27	Shaikh	Series IV.3	Rect	8.0	6.00	8.00	6.00	4.00	48.0	256	5880	830	**4370**
28	Warwaruk, Sozen	OB.24.168	Rect	12.2	6.10	12.20	6.10	6.10	74.4	923	3450	420	**3350**
29	Warwaruk, Sozen	OB.24.189	Rect	12.0	6.20	12.00	6.20	6.00	74.4	893	4280	510	**3730**
30	Warwaruk, Sozen	OB.34.038	Rect	12.1	6.00	12.10	6.00	6.05	72.6	886	8320	540	**5200**
31	Warwaruk, Sozen	OB.34.043	Rect	12.1	6.10	12.10	6.10	6.05	73.8	901	6560	710	**4620**
32	Warwaruk, Sozen	OB.34.071	Rect	12.1	6.00	12.10	6.00	6.05	72.6	886	7180	545	**4830**
33	Warwaruk, Sozen	OB.34.073	Rect	12.1	6.10	12.10	6.10	6.05	73.8	901	3820	495	**3520**
34	Warwaruk, Sozen	OB.34.074	Rect	12.1	6.10	12.10	6.10	6.05	73.8	901	7630	710	**4980**
35	Warwaruk, Sozen	OB.34.076	Rect	12.0	6.00	12.00	6.00	6.00	72.0	864	5490	560	**4220**
36	Warwaruk, Sozen	OB.34.077	Rect	12.1	6.10	12.10	6.10	6.05	73.8	901	5650	805	**4280**
37	Warwaruk, Sozen	OB.34.115	Rect	12.0	6.00	12.00	6.00	6.00	72.0	864	8200	605	**5160**
38	Warwaruk, Sozen	OB.34.120	Rect	12.1	6.10	12.10	6.10	6.05	73.8	901	3440	615	**3340**
39	Warwaruk, Sozen	OB.34.122	Rect	12.0	6.10	12.00	6.10	6.00	73.2	878	6120	660	**4460**
40	Warwaruk, Sozen	OB.34.159	Rect	12.1	6.10	12.10	6.10	6.05	73.8	901	5910	750	**4380**
41	Warwaruk, Sozen	OB.34.196	Rect	12.0	6.10	12.00	6.10	6.00	73.2	878	3270	515	**3260**
42	Warwaruk, Sozen	OB.34.200	Rect	12.1	6.10	12.10	6.10	6.05	73.8	901	4590	580	**3860**
43	Warwaruk, Sozen	OB.34.290	Rect	12.1	6.10	12.10	6.10	6.05	73.8	901	3280	475	**3260**
44	Warwaruk, Sozen	OB.44.140	Rect	12.1	6.10	12.10	6.10	6.05	73.8	901	6220	600	**4500**
45	Warwaruk, Sozen	OB.44.158	Rect	12.0	6.00	12.00	6.00	6.00	72.0	864	4100	560	**3650**
46	Warwaruk, Sozen	RB.34.093	Rect	12.0	6.30	12.00	6.30	6.00	75.6	907	3970	390	**3590**
47	Warwaruk, Sozen	RB.34.126	Rect	12.0	6.10	12.00	6.10	6.00	73.2	878	5230	420	**4120**
48	Sozen	A.11.43	Rect	12.0	6.00	12.00	6.00	6.00	72.0	864	6220	704	**4500**
49	Sozen	A.11.53	Rect	12.0	6.00	12.00	6.00	6.00	72.0	864	4360	596	**3760**
50	Sozen	A.12.23	Rect	12.0	6.10	12.00	6.10	6.00	73.2	878	5650	805	**4280**
51	Sozen	A.12.31	Rect	12.0	6.00	12.00	6.00	6.00	72.0	864	5800	514	**4340**
52	Sozen	A.12.34	Rect	12.0	6.00	12.00	6.00	6.00	72.0	864	7990	835	**5100**
53	Sozen	A.12.36	Rect	12.0	6.10	12.00	6.10	6.00	73.2	878	3440	615	**3340**

NOTES:

E_c used is **Bold** if calculated using the reported $f'_{c,test}$ value. Otherwise, E_c is the value reported in the primary source.

Table C-1: Specimen Identification, Cross-Sectional Properties, and Concrete Material Properties (Cont.)

Ref #	Reference Author(s)	Beam ID	Cross Section Type	h (in.)	b_f (in.)	h_f (in.)	b_w (in.)	$y_{t,gross}$ (in.)	A_g (in.^{2})	I_g (in.^{4})	$f'_{c,test}$ (psi)	$f_{r,reported}$ (psi)	E_c used (ksi)
54	Sozen	A.12.42	Rect	12.0	6.00	12.00	6.00	6.00	72.0	864	6260	773	**4510**
55	Sozen	A.12.46	Rect	12.0	6.00	12.00	6.00	6.00	72.0	864	4660	596	**3890**
56	Sozen	A.12.48	Rect	12.0	6.00	12.00	6.00	6.00	72.0	864	4840	606	**3970**
57	Sozen	A.12.53	Rect	12.0	6.00	12.00	6.00	6.00	72.0	864	3400	342	**3320**
58	Sozen	A.12.56	Rect	12.0	6.00	12.00	6.00	6.00	72.0	864	3790	533	**3510**
59	Sozen	A.12.60	Rect	12.0	6.00	12.00	6.00	6.00	72.0	864	3350	542	**3300**
60	Sozen	A.12.73	Rect	12.0	6.00	12.00	6.00	6.00	72.0	864	3550	580	**3400**
61	Sozen	A.14.39	Rect	12.0	6.00	12.00	6.00	6.00	72.0	864	3350	509	**3300**
62	Sozen	A.14.44	Rect	12.0	6.00	12.00	6.00	6.00	72.0	864	3350	377	**3300**
63	Sozen	A.14.55	Rect	12.0	6.00	12.00	6.00	6.00	72.0	864	3320	434	**3280**
64	Sozen	A.21.39	Rect	12.0	6.00	12.00	6.00	6.00	72.0	864	3130	519	**3190**
65	Sozen	A.21.51	Rect	12.0	6.00	12.00	6.00	6.00	72.0	864	5630	642	**4280**
66	Sozen	A.22.40	Rect	12.0	6.00	12.00	6.00	6.00	72.0	864	5790	748	**4340**
67	Sozen	A.22.49	Rect	12.0	6.00	12.00	6.00	6.00	72.0	864	4760	670	**3930**
68	Sozen	B.11.07	I	12.0	6.05	2.65	3.02	6.00	50.8	811	8260	585	**5180**
69	Sozen	B.11.20	I	12.0	5.92	2.65	2.95	6.00	49.7	793	4525	510	**3830**
70	Sozen	B.11.29	I	12.0	5.95	2.65	2.95	6.00	49.9	797	4190	450	**3690**
71	Sozen	B.12.12	I	12.0	6.00	2.65	3.00	6.00	50.4	804	4570	420	**3850**
72	Sozen	B.12.14	I	12.0	6.00	2.65	3.00	6.00	50.4	804	3850	390	**3540**
73	Sozen	B.12.26	I	12.0	6.14	2.65	3.03	6.00	51.4	822	4460	300	**3810**
74	Sozen	B.12.29	I	12.0	6.00	2.65	3.00	6.00	50.4	804	4180	430	**3690**
75	Sozen	B.12.35	I	12.0	6.30	2.65	3.08	6.00	52.6	843	3210	400	**3230**
76	Sozen	B.13.16	I	12.0	6.00	2.65	3.00	6.00	50.4	804	5540	570	**4240**
77	Sozen	B.21.26	I	12.0	6.00	2.65	2.96	6.00	50.2	803	4470	510	**3810**
78	Sozen	B.22.23	I	12.0	6.05	2.65	3.00	6.00	50.7	810	5120	390	**4080**
79	Sozen	C.12.18	I	12.0	6.00	2.75	1.75	6.00	45.8	796	5310	460	**4150**
80	Sozen	C.12.19	I	12.0	6.00	2.75	1.79	6.00	46.0	796	6040	400	**4430**
81	Hernandez	G1	I	12.0	6.00	2.75	1.70	6.00	44.7	795	3100	442	**3170**

NOTES:

E_c used is **Bold** if calculated using the reported $f'_{c,test}$ value. Otherwise, E_c is the value reported in the primary source.

Table C-1: Specimen Identification, Cross-Sectional Properties, and Concrete Material Properties (Cont.)

Ref #	Reference Author(s)	Beam ID	Cross Section Type	h (in.)	b_f (in.)	h_f (in.)	b_w (in.)	$y_{t,gross}$ (in.)	A_g (in.^{2})	I_g (in.^{4})	$f'_{c,test}$ (psi)	$f_{r,reported}$ (psi)	Ec used (ksi)
82	Hernandez	G2	I	12.0	6.00	2.75	1.70	6.00	44.7	795	3280	433	**3260**
83	Hernandez	G5	I	12.0	5.95	2.75	1.70	6.00	44.4	788	3240	425	**3240**
84	Hernandez	G7	I	12.0	5.95	2.75	1.71	6.00	44.5	788	4660	458	**3890**
85	Hernandez	G9	I	12.0	6.00	2.75	1.78	6.00	45.1	796	3080	366	**3160**
86	Hernandez	G11	I	12.0	6.00	2.75	1.70	6.00	44.7	795	3020	400	**3130**
87	Hernandez	G12	I	12.0	5.95	2.65	2.90	6.00	49.6	796	3050	392	**3150**
88	Hernandez	G13	I	12.0	6.00	2.75	1.76	6.00	45.0	796	3140	371	**3190**
89	Hernandez	G14	I	12.0	6.00	2.65	2.95	6.00	50.1	803	3110	316	**3180**
90	Hernandez	G16	I	12.0	5.98	2.65	2.96	6.00	50.1	801	3810	342	**3520**
91	Hernandez	G22	I	12.0	6.00	2.75	1.80	6.00	45.2	796	3300	425	**3270**
92	Hernandez	G24	I	12.0	6.00	2.75	1.75	6.00	44.9	796	3010	383	**3130**
93	Hernandez	G25	I	12.0	6.00	2.75	1.75	6.00	44.9	796	3230	396	**3240**
94	Hernandez	G27	I	12.0	6.00	2.75	1.80	6.00	45.2	796	5050	492	**4050**
95	Hernandez	G28	I	12.0	6.00	2.65	3.00	6.00	50.4	804	3870	425	**3550**
96	Hernandez	G29	I	12.0	6.00	2.75	1.75	6.00	44.9	796	4330	433	**3750**
97	Hernandez	G30	I	12.0	6.00	2.65	3.00	6.00	50.4	804	5430	475	**4200**
98	Hernandez	G31	I	12.0	6.00	2.65	3.00	6.00	50.4	804	3160	267	**3200**
99	Hernandez	G35	I	12.0	6.00	2.65	3.00	6.00	50.4	804	3550	392	**3400**
100	Hernandez	G37	I	12.0	6.00	2.65	3.00	6.00	50.4	804	3210	392	**3230**
101	Janney et al.	1-0.141	Rect	12.0	6.00	12.00	6.00	6.00	72.0	864	5350	NR	**4170**
102	Janney et al.	1-0.250	Rect	12.0	6.00	12.00	6.00	6.00	72.0	864	6050	NR	**4430**
103	Janney et al.	1-0.420	Rect	12.0	6.00	12.00	6.00	6.00	72.0	864	5400	NR	**4190**
104	Janney et al.	2-0.151	Rect	12.0	6.00	12.00	6.00	6.00	72.0	864	5000	NR	**4030**
105	Janney et al.	2-0.306	Rect	12.0	6.00	12.00	6.00	6.00	72.0	864	4950	NR	**4010**
106	Janney et al.	2-0.398	Rect	12.0	6.00	12.00	6.00	6.00	72.0	864	5700	NR	**4300**

NOTES:

E_c used is **Bold** if calculated using the reported $f'_{c,test}$ value. Otherwise, E_c is the value reported in the primary source.

Table C-2: Specimen Reinforcement Properties

	Prestressed Reinforcement							Nonprestressed Tension Reinforcement						Nonprestressed Compression Reinforcement		
Ref #	PRE/POST tensioned?	f_{pu} (ksi)	Ø (in.)	A_p (in.^{2})	d_p (in.)	$f_{pe,w}$ (ksi)	f_{ps} (ksi)	f_y (ksi)	# of bars	Ø (in.)	A_s (in.^{2})	L_s (ft)	d_s (in.)	f_y (ksi)	A'_s (in.^{2})	d'_s (in.^{2})
1	PRE	270	0.5 sp	0.167	4.50	185	266	-	-	-	-	-	-	-	-	-
2	PRE	270	0.500	0.918	7.50	136	225	-	-	-	-	-	-	-	-	-
3	PRE	270	0.500	0.918	7.50	138	230	-	-	-	-	-	-	-	-	-
4	PRE	270	0.500	0.918	7.50	135	232	-	-	-	-	-	-	-	-	-
5	PRE	270	0.5 sp	3.340	20.37	159	269	-	-	-	-	-	-	-	-	-
6	PRE	270	0.5625 sp	2.688	22.00	174	269	60	1	0.75	0.44	20	25	-	-	-
7	PRE	270	0.5625 sp	2.304	24.18	175	269	60	1	0.875	0.6	24	23	-	-	-
8	PRE	270	0.500	0.612	24.00	176	268	60	3	0.625	0.93	-	26.4	-	-	-
9	PRE	270	0.500	0.612	24.00	176	266	60	3	1	2.37	-	26	-	-	-
10	PRE	270	0.500	1.071	24.00	103	266	-	-	-	-	-	-	-	-	-
11	PRE	270	0.500	1.071	24.00	103	262	60	4 1	0.625 0.875	1.84	-	26.15	-	-	-
12	PRE	270	0.500	1.071	24.00	103	260	60	3	1	2.37	-	26	-	-	-
13	PRE	270	0.500	1.530	24.00	73	259	-	-	-	-	-	-	-	-	-
14	PRE	270	0.500	1.530	24.00	73	250	60	1 2	0.625 0.875	1.51	-	26.09	-	-	-
15	PRE	270	0.500	1.530	24.00	73	240	60	3	1	2.37	-	26	-	-	-
16	PRE	250	0.313	0.173	6.50	135	241	33	1	0.5	0.2	-	5.25	-	-	-
17	PRE	250	0.313	0.173	6.50	130	237	33	2	0.5	0.4	-	5.25	-	-	-
18	PRE	250	0.313	0.173	6.50	138	234	33	3	0.5	0.6	-	5.25	-	-	-
19	PRE	250	0.313	0.116	6.50	141	244	250	1	0.3125	0.058	-	6.5	-	-	-
20	PRE	250	0.313	0.116	6.50	141	244	60	1	0.5	0.2	-	6.5	-	-	-
21	PRE	250	0.313	0.116	6.50	142	244	33	2	0.5	0.4	-	5.88	-	-	-
22	PRE	250	0.375	0.240	6.50	91	221	33	1	0.625	0.31	-	5.25	-	-	-
23	PRE	250	0.313	0.173	6.50	136	244	-	-	-	-	-	-	-	-	-
24	PRE	250	0.375	0.240	6.50	89	233	-	-	-	-	-	-	-	-	-
25	PRE	250	0.375	0.160	6.50	121	239	250	1	0.375	0.08	-	6.5	-	-	-

NOTES: “sp” stands for special strand size.

Table C-2: Specimen Reinforcement Properties (Cont.)

	Prestressed Reinforcement							Nonprestressed Tension Reinforcement						Nonprestressed Compression Reinforcement		
Ref #	PRE/POST tensioned?	f_{pu} (ksi)	Ø (in.)	A_p (in.^{2})	d_p (in.)	$f_{pe,w}$ (ksi)	f_{ps} (ksi)	f_y (ksi)	# of strands	Ø (in.)	A_s (in.^{2})	L_s (ft)	d_s (in.)	f_y (ksi)	A'_s (in.^{2})	d'_s (in.^{2})
26	PRE	250	0.375	0.160	6.50	122	236	60	1	0.625	0.31	-	6.5	-	-	-
27	PRE	250	0.375	0.160	6.50	119	235	33	3	0.5	0.6	-	5.67	-	-	-
28	POST	250	0.192	0.290	8.23	100	203	-	-	-	-	-	-	-	-	-
29	POST	250	0.192	0.405	8.07	100	191	-	-	-	-	-	-	-	-	-
30	POST	250	0.191	0.171	9.08	120	247	-	-	-	-	-	-	-	-	-
31	POST	250	0.199	0.157	9.05	118	247	-	-	-	-	-	-	-	-	-
32	POST	250	0.191	0.285	9.32	120	242	-	-	-	-	-	-	-	-	-
33	POST	250	0.199	0.156	9.27	119	244	-	-	-	-	-	-	-	-	-
34	POST	250	0.199	0.311	9.13	115	241	-	-	-	-	-	-	-	-	-
35	POST	250	0.192	0.232	9.11	108	242	-	-	-	-	-	-	-	-	-
36	POST	250	0.199	0.249	9.33	114	242	-	-	-	-	-	-	-	-	-
37	POST	250	0.199	0.467	8.20	117	221	-	-	-	-	-	-	-	-	-
38	POST	250	0.192	0.232	9.19	114	234	-	-	-	-	-	-	-	-	-
39	POST	250	0.199	0.373	8.24	116	227	-	-	-	-	-	-	-	-	-
40	POST	250	0.199	0.467	8.09	113	204	-	-	-	-	-	-	-	-	-
41	POST	250	0.199	0.311	8.01	115	197	-	-	-	-	-	-	-	-	-
42	POST	250	0.199	0.467	8.36	118	195	-	-	-	-	-	-	-	-	-
43	POST	250	0.199	0.467	7.99	113	165	-	-	-	-	-	-	-	-	-
44	POST	250	0.193	0.439	8.27	151	230	-	-	-	-	-	-	-	-	-
45	POST	250	0.193	0.322	8.29	149	230	-	-	-	-	-	-	-	-	-
46	PRE	250	0.196	0.211	9.06	114	241	-	-	-	-	-	-	-	-	-
47	PRE	250	0.196	0.362	9.08	112	228	-	-	-	-	-	-	-	-	-
48	POST	250	0.193	0.440	8.24	116	214	-	-	-	-	-	-	-	-	-
49	POST	250	0.199	0.373	8.02	125	210	-	-	-	-	-	-	-	-	-
50	POST	250	0.199	0.249	9.33	114	242	-	-	-	-	-	-	-	-	-
51	PRE	250	0.199	0.311	8.64	114	235	-	-	-	-	-	-	-	-	-
52	POST	250	0.193	0.440	8.20	110	221	-	-	-	-	-	-	-	-	-

NOTES: “sp” stands for special strand size.

Table C-2: Specimen Reinforcement Properties (Cont.)

	Prestressed Reinforcement							Nonprestressed Tension Reinforcement						Nonprestressed Compression Reinforcement		
Ref #	PRE/POST tensioned?	f_{pu} (ksi)	Ø (in.)	A_p (in.^{2})	d_p (in.)	$f_{pe,w}$ (ksi)	f_{ps} (ksi)	f_y (ksi)	# of strands	Ø (in.)	A_s (in.^{2})	L_s (ft)	d_s (in.)	f_y (ksi)	A'_s (in.^{2})	d'_s (in.^{2})
53	POST	250	0.192	0.232	9.19	114	234	-	-	-	-	-	-	-	-	-
54	POST	250	0.193	0.440	8.30	103	208	-	-	-	-	-	-	-	-	-
55	POST	250	0.193	0.352	8.20	131	224	-	-	-	-	-	-	-	-	-
56	POST	250	0.193	0.381	8.20	140	224	-	-	-	-	-	-	-	-	-
57	PRE	250	0.199	0.311	8.60	108	203	-	-	-	-	-	-	-	-	-
58	PRE	250	0.196	0.362	8.59	121	206	-	-	-	-	-	-	-	-	-
59	POST	250	0.193	0.352	8.81	136	210	-	-	-	-	-	-	-	-	-
60	POST	250	0.193	0.440	8.44	104	174	-	-	-	-	-	-	-	-	-
61	POST	250	0.199	0.218	8.35	117	231	-	-	-	-	-	-	-	-	-
62	POST	250	0.199	0.249	8.50	118	224	-	-	-	-	-	-	-	-	-
63	POST	250	0.199	0.311	8.53	117	205	-	-	-	-	-	-	-	-	-
64	POST	250	0.199	0.218	8.95	59	208	-	-	-	-	-	-	-	-	-
65	POST	250	0.199	0.467	8.12	59	171	-	-	-	-	-	-	-	-	-
66	POST	250	0.193	0.381	8.20	72	199	-	-	-	-	-	-	-	-	-
67	POST	250	0.193	0.381	8.20	57	179	-	-	-	-	-	-	-	-	-
68	PRE	250	0.196	0.121	11.07	122	248	-	-	-	-	-	-	-	-	-
69	PRE	250	0.195	0.178	10.21	124	245	-	-	-	-	-	-	-	-	-
70	PRE	250	0.195	0.239	10.00	124	241	-	-	-	-	-	-	-	-	-
71	PRE	250	0.196	0.121	11.13	125	248	-	-	-	-	-	-	-	-	-
72	PRE	250	0.196	0.121	11.14	123	247	-	-	-	-	-	-	-	-	-
73	PRE	250	0.193	0.233	10.06	110	242	-	-	-	-	-	-	-	-	-
74	PRE	250	0.195	0.238	9.76	122	241	-	-	-	-	-	-	-	-	-
75	PRE	250	0.195	0.238	9.99	121	236	-	-	-	-	-	-	-	-	-
76	PRE	250	0.195	0.179	10.38	126	246	-	-	-	-	-	-	-	-	-
77	PRE	250	0.195	0.238	10.21	62	237	-	-	-	-	-	-	-	-	-
78	PRE	250	0.195	0.238	10.03	55	239	-	-	-	-	-	-	-	-	-
79	PRE	250	0.199	0.187	9.69	114	245	-	-	-	-	-	-	-	-	-

NOTES: “sp” stands for special strand size.

Table C-2: Specimen Reinforcement Properties (Cont.)

	Prestressed Reinforcement							Nonprestressed Tension Reinforcement						Nonprestressed Compression Reinforcement		
Ref #	PRE/POST tensioned?	f_{pu} (ksi)	Ø (in.)	A_p (in.^{2})	d_p (in.)	$f_{pe,w}$ (ksi)	f_{ps} (ksi)	f_y (ksi)	# of strands	Ø (in.)	A_s (in.^{2})	L_s (ft)	d_s (in.)	f_y (ksi)	A'_s (in.^{2})	d'_s (in.^{2})
80	PRE	250	0.193	0.233	10.11	111	244	-	-	-	-	-	-	-	-	-
81	PRE	250	0.196	0.121	10.50	126	246	-	-	-	-	-	-	-	-	-
82	PRE	250	0.196	0.121	10.50	126	246	-	-	-	-	-	-	-	-	-
83	PRE	250	0.196	0.242	10.11	121	235	-	-	-	-	-	-	-	-	-
84	PRE	250	0.196	0.242	10.14	122	242	-	-	-	-	-	-	-	-	-
85	PRE	250	0.196	0.121	10.48	126	246	-	-	-	-	-	-	-	-	-
86	PRE	250	0.196	0.121	10.49	127	246	-	-	-	-	-	-	-	-	-
87	PRE	250	0.196	0.242	10.11	121	232	-	-	-	-	-	-	-	-	-
88	PRE	250	0.196	0.121	10.49	126	246	-	-	-	-	-	-	-	-	-
89	PRE	250	0.196	0.242	10.11	120	233	-	-	-	-	-	-	-	-	-
90	PRE	250	0.196	0.242	10.14	121	240	-	-	-	-	-	-	-	-	-
91	PRE	250	0.196	0.242	10.11	113	234	-	-	-	-	-	-	-	-	-
92	PRE	250	0.196	0.242	10.14	120	232	-	-	-	-	-	-	-	-	-
93	PRE	250	0.196	0.121	10.47	127	246	-	-	-	-	-	-	-	-	-
94	PRE	250	0.196	0.242	10.15	121	243	-	-	-	-	-	-	-	-	-
95	PRE	250	0.196	0.242	10.02	117	239	-	-	-	-	-	-	-	-	-
96	PRE	250	0.196	0.242	10.03	119	241	-	-	-	-	-	-	-	-	-
97	PRE	250	0.196	0.242	10.10	120	244	-	-	-	-	-	-	-	-	-
98	PRE	250	0.196	0.242	10.05	122	234	-	-	-	-	-	-	-	-	-
99	PRE	250	0.196	0.242	10.15	122	238	-	-	-	-	-	-	-	-	-
100	PRE	250	0.196	0.242	10.12	123	235	-	-	-	-	-	-	-	-	-
101	PRE	250	0.375	0.160	8.30	119	245	-	-	-	-	-	-	-	-	-
102	PRE	250	0.375	0.320	8.30	113	234	-	-	-	-	-	-	-	-	-
103	PRE	250	0.375	0.480	8.30	117	201	-	-	-	-	-	-	-	-	-
104	POST	250	0.375	0.160	8.30	126	245	-	-	-	-	-	-	-	-	-
105	POST	250	0.375	0.320	8.30	118	229	-	-	-	-	-	-	-	-	-
106	POST	250	0.375	0.480	8.30	117	204	-	-	-	-	-	-	-	-	-

NOTES: “sp” stands for special strand size.

Table C-3: Specimen Span and Loading Geometry, Midspan Bending Moments, and ACI 318 Prestressing Classification

Ref #	L (ft)	L_{Total} (ft)	PL #	a (in.)	M_w (kip-in)	M_{dec} (kip-in)	$M_{TOTAL,6}$ (kip-in)	$M_{TOTAL,7.5}$ (kip-in)	$M_{TOTAL,10}$ (kip-in)	$M_{TOTAL,12}$ (kip-in)	$M_{TOTAL,0.6}$ (kip-in)	$2/3M_n$ (kip-in)	$2/3M_F$ (kip-in)	M_V (kip-in)	CLASS
1	11.50	11.83	2	57.0	10	79	107	114	126	136	286	***123***	-	-	T
2	14.50	15.00	2	75.0	22	613	685	703	733	757	969	***848***	-	-	C
3	14.50	15.00	2	75.0	24	606	685	705	737	764	1030	***871***	-	-	C
4	14.50	15.00	2	75.0	26	580	666	688	723	752	1092	***884***	-	-	C
5	62.00	62.67	0	N/A	5473	8815	10175	10515	11082	11535	34618	***11843***	-	-	C
6	62.00	62.50	0	N/A	5138	8745	9919	10212	10701	11093	32444	***10789***	-	-	T
7	62.00	62.67	0	N/A	5645	8121	9775	10188	10877	11428	41942	***10392***	-	-	T
8	13.33	15.33	1	80.0	110	1610	2655	2917	3352	3701	9445	***3432***	4133	4834	T
9	13.33	15.33	1	80.0	112	1603	2717	2995	3459	3831	9820	4753	***4525***	5353	C
10	13.33	15.33	1	80.0	107	1671	2682	2935	3357	3694	9430	***4269***	4475	4641	C
11	13.33	15.33	1	80.0	108	1662	2737	3006	3454	3812	9498	5871	5832	***5350***	C
12	13.33	15.33	1	80.0	106	1659	2735	3004	3452	3810	9395	6282	***4865***	5555	C
13	13.33	15.33	1	80.0	108	1707	2714	2966	3386	3721	9105	5774	***4975***	5308	C
14	13.33	15.33	1	80.0	108	1698	2759	3025	3467	3821	9272	6876	***5397***	5442	C
15	13.33	15.33	1	80.0	108	1692	2784	3057	3512	3876	9357	7390	***5264***	5842	C
16	15.00	15.50	2	66.0	17	92	121	129	141	151	237	***175***	-	-	C
17	15.00	15.50	2	66.0	17	87	117	125	137	147	236	***188***	-	-	C
18	15.00	15.50	2	66.0	17	91	122	129	142	152	238	***201***	-	-	C
19	15.00	15.50	2	66.0	17	64	94	102	115	125	248	***160***	-	-	C
20	15.00	15.50	2	66.0	17	64	95	103	116	126	249	***157***	-	-	C
21	15.00	15.50	2	66.0	17	63	95	102	116	126	248	***155***	-	-	C
22	15.00	15.50	2	66.0	17	86	119	127	141	152	281	***226***	-	-	C
23	15.00	15.50	2	66.0	17	93	125	133	147	157	282	***165***	-	-	C
24	15.00	15.50	2	66.0	17	86	118	127	140	151	281	***211***	-	-	C
25	15.00	15.50	2	66.0	17	76	107	115	128	138	251	***193***	-	-	C
26	15.00	15.50	2	66.0	17	76	108	117	130	141	254	***209***	-	-	C
27	15.00	15.50	2	66.0	17	73	105	113	127	137	251	***201***	-	-	C
28	9.00	10.00	2	34.0	9	124	178	192	214	233	316	258	***247***	-	C
29	9.00	10.00	2	34.0	9	170	230	245	270	290	385	327	***277***	-	T

NOTES: Value of maximum feasible service-level bending moment (used to determine classification) is **bold**.

Table C-3: Specimen Span and Loading Geometry, Midspan Bending Moments, and ACI 318 Prestressing Classification (Cont.)

Ref #	L (ft)	L_{Total} (ft)	PL #	a (in.)	M_w (kip-in)	M_{dec} (kip-in)	$M_{TOTAL,6}$ (kip-in)	$M_{TOTAL,7.5}$ (kip-in)	$M_{TOTAL,10}$ (kip-in)	$M_{TOTAL,12}$ (kip-in)	$M_{TOTAL,0.6}$ (kip-in)	$2/3M_n$ (kip-in)	$2/3M_F$ (kip-in)	M_V (kip-in)	CLASS
30	9.00	10.00	2	34.0	9	105	186	207	241	268	754	242	***236***	-	T
31	9.00	10.00	2	34.0	9	94	167	186	216	241	606	218	***194***	-	T
32	9.00	10.00	2	34.0	9	187	263	282	314	340	678	386	***359***	-	C
33	9.00	10.00	2	34.0	9	99	155	169	193	212	365	211	***180***	-	T
34	9.00	10.00	2	34.0	9	188	268	288	322	348	723	409	***376***	-	C
35	9.00	10.00	2	34.0	9	131	197	213	241	263	505	304	***281***	-	C
36	9.00	10.00	2	34.0	9	155	224	241	270	293	544	334	***315***	-	C
37	9.00	10.00	2	34.0	9	237	317	337	370	397	720	480	***446***	-	C
38	9.00	10.00	2	34.0	9	141	195	208	231	249	339	277	***251***	-	C
39	9.00	10.00	2	34.0	9	189	259	277	306	330	549	390	***364***	-	C
40	9.00	10.00	2	34.0	9	220	290	308	337	361	529	415	***408***	-	C
41	9.00	10.00	2	34.0	9	146	198	211	232	249	288	***254***	273	-	C
42	9.00	10.00	2	34.0	9	248	310	326	352	373	427	392	***372***	-	T
43	9.00	10.00	2	34.0	9	216	269	282	304	322	289	***294***	357	-	T
44	9.00	10.00	2	34.0	9	290	362	380	411	435	570	452	***401***	-	T
45	9.00	10.00	2	34.0	9	212	268	283	306	325	369	322	***294***	-	T
46	9.00	11.00	2	32.0	9	125	184	198	223	242	388	267	***217***	-	T
47	9.00	11.00	2	32.0	9	216	282	298	325	347	507	416	***334***	-	T
48	9.00	10.42	1	54.0	9	224	293	311	340	363	551	***424***	449	522	C
49	9.00	10.42	1	54.0	9	192	250	265	289	309	378	***327***	389	468	C
50	9.00	10.42	2	36.0	9	156	224	241	270	292	538	334	***331***	423	C
51	9.00	10.83	2	36.0	9	169	237	254	282	304	526	361	***326***	369	C
52	9.00	10.42	2	36.0	9	209	288	308	341	367	701	454	***405***	513	C
53	9.00	10.42	2	36.0	9	142	195	209	231	249	336	277	***266***	383	C
54	9.00	10.42	2	36.0	9	202	272	290	319	343	556	419	***379***	495	C
55	9.00	10.42	2	36.0	9	200	260	275	301	321	412	343	***337***	423	C
56	9.00	10.42	2	36.0	9	231	293	308	334	354	429	368	***367***	-	C
57	9.00	10.83	2	36.0	9	161	213	226	247	265	315	***285***	302	333	C
58	9.00	10.83	2	36.0	9	208	264	277	300	319	355	331	***324***	405	C

NOTES: Value of maximum feasible service-level bending moment (used to determine classification) is **bold**.

Table C-3: Specimen Span and Loading Geometry, Midspan Bending Moments, and ACI 318 Prestressing Classification (Cont.)

Ref #	L (ft)	L_{Total} (ft)	PL #	a (in.)	M_w (kip-in)	M_{dec} (kip-in)	$M_{TOTAL,6}$ (kip-in)	$M_{TOTAL,7.5}$ (kip-in)	$M_{TOTAL,10}$ (kip-in)	$M_{TOTAL,12}$ (kip-in)	$M_{TOTAL,0.6}$ (kip-in)	$2/3M_n$ (kip-in)	$2/3M_F$ (kip-in)	M_V (kip-in)	CLASS
59	9.00	10.42	2	36.0	9	241	293	306	328	345	331	***328***	333	495	T
60	9.00	10.42	2	36.0	9	213	267	280	303	320	328	***323***	346	423	C
61	7.00	10.42	2	24.0	4	114	164	177	198	215	299	***231***	234	340	C
62	7.00	10.42	2	24.0	4	136	187	200	221	238	305	***256***	259	334	C
63	7.00	10.42	2	24.0	4	171	222	235	257	274	307	***283***	319	400	C
64	9.00	10.42	1	54.0	9	65	115	128	148	165	284	227	***203***	225	C
65	9.00	10.42	1	54.0	9	117	184	201	228	250	490	358	***318***	387	C
66	9.00	10.42	2	36.0	9	118	186	202	230	253	506	350	***321***	387	C
67	9.00	10.42	2	36.0	9	94	155	170	195	216	416	309	***284***	297	C
68	9.00	10.83	1	54.0	6	117	193	212	243	268	711	***215***	233	345	T
69	9.00	10.83	1	54.0	6	158	214	228	251	269	397	269	***251***	330	T
70	9.00	10.83	1	54.0	6	210	264	278	300	318	378	332	***316***	371	T
71	9.00	10.83	2	36.0	6	123	179	193	217	236	410	209	***209***	274	T
72	9.00	10.83	2	36.0	6	121	173	186	208	225	351	***207***	210	260	T
73	9.00	10.83	2	36.0	6	182	240	254	278	298	407	333	***276***	336	T
74	9.00	10.83	2	36.0	6	196	251	264	287	305	371	321	***309***	359	C
75	9.00	10.83	2	36.0	6	204	255	268	289	305	312	313	***278***	330	T
76	9.00	10.83	2	28.0	6	165	227	243	269	290	489	282	***254***	352	T
77	9.00	10.83	1	54.0	6	108	165	179	203	222	387	338	***228***	237	C
78	9.00	10.83	2	36.0	6	93	153	169	194	214	437	340	***230***	237	C
79	9.00	10.83	2	36.0	6	145	205	220	245	265	441	270	***222***	267	T
80	9.00	10.83	2	36.0	6	191	256	272	299	320	517	349	***274***	312	T
81	9.00	10.83	2	36.0	5	118	164	176	195	210	272	***190***	197	239	T
82	9.00	10.83	2	36.0	5	118	166	177	197	213	286	***191***	197	230	T
83	9.00	10.83	2	36.0	5	223	271	283	303	319	292	317	***310***	344	T
84	9.00	10.83	2	36.0	5	223	279	294	317	336	406	348	***331***	346	T
85	9.00	10.83	2	36.0	5	118	164	176	195	210	271	***189***	197	256	T
86	9.00	10.83	2	36.0	5	120	165	177	196	211	266	***189***	197	238	T
87	9.00	10.83	2	36.0	6	213	260	272	291	307	289	***311***	319	384	C

NOTES: Value of maximum feasible service-level bending moment (used to determine classification) is **bold**.

Table C-3: Specimen Span and Loading Geometry, Midspan Bending Moments, and ACI 318 Prestressing Classification (Cont.)

Ref #	L (ft)	L_{Total} (ft)	PL #	a (in.)	M_w (kip-in)	M_{dec} (kip-in)	$M_{TOTAL,6}$ (kip-in)	$M_{TOTAL,7.5}$ (kip-in)	$M_{TOTAL,10}$ (kip-in)	$M_{TOTAL,12}$ (kip-in)	$M_{TOTAL,0.6}$ (kip-in)	$2/3M_n$ (kip-in)	$2/3M_F$ (kip-in)	M_V (kip-in)	CLASS
88	9.00	10.83	2	36.0	5	118	165	176	196	211	276	190	***189***	229	T
89	9.00	10.83	2	36.0	6	212	259	271	291	307	296	***314***	318	380	C
90	9.00	10.83	2	36.0	6	213	265	278	300	318	353	334	***293***	361	T
91	9.00	10.83	2	36.0	5	207	255	268	288	304	298	319	321	***317***	C
92	9.00	10.83	2	36.0	5	223	270	281	301	316	277	***312***	315	335	T
93	9.00	10.83	2	36.0	5	119	166	178	198	213	283	***190***	193	248	T
94	9.00	10.83	2	36.0	5	221	281	296	320	340	442	353	***342***	403	C
95	9.00	10.83	2	36.0	6	201	254	267	289	307	354	330	***318***	373	C
96	9.00	10.83	2	28.0	5	213	268	282	305	324	379	339	331	***283***	T
97	9.00	10.83	2	36.0	6	207	269	284	310	331	483	355	***340***	460	C
98	9.00	10.83	1	54.0	6	212	260	272	292	309	299	***313***	327	368	C
99	9.00	10.83	2	48.0	6	216	267	280	301	318	334	329	***315***	419	T
100	9.00	10.83	2	48.0	6	216	264	276	297	313	306	318	***313***	457	T
101	9.00	10.00	2	36.0	9	83	147	163	189	211	468	***198***	-	-	T
102	9.00	10.00	2	36.0	9	159	228	245	273	296	534	***354***	-	-	C
103	9.00	10.00	2	36.0	9	251	316	333	360	382	485	***421***	-	-	C
104	9.00	10.00	2	36.0	9	88	150	165	191	211	438	***197***	-	-	T
105	9.00	10.00	2	36.0	9	167	229	244	270	291	440	***334***	-	-	C
106	9.00	10.00	2	36.0	9	251	318	335	363	385	510	***432***	-	-	C

NOTES: Value of maximum feasible service-level bending moment (used to determine classification) is **bold**.

Table C-4: Midspan Deflections (from original sources) for Specific Levels of Midspan Bending Moment

Ref #	$\Delta_{test,6}$ (in.)	$\Delta_{test,7.5}$ (in.)	$\Delta_{test,10}$ (in.)	$\Delta_{test,12}$ (in.)	$\Delta_{test,max}$ (in.)
1	0.34	0.38	*0.49*	*0.61*	0.43
2	0.42	0.44	0.46	0.48	0.60
3	0.40	0.41	0.44	0.46	0.61
4	0.37	0.38	0.40	0.42	0.56
5	0.84	0.95	1.32	1.74	2.08
6	1.33	1.46	1.76	*2.19*	1.85
7	0.68	0.76	*1.11*	*1.62*	0.81
8	0.051	0.059	0.076	*0.100*	0.082
9	0.046	0.054	0.070	0.086	0.133
10	0.047	0.058	0.082	0.117	0.238
11	0.045	0.050	0.063	0.078	0.215
12	0.045	0.050	0.063	0.076	0.137
13	0.055	0.064	0.082	0.101	0.301
14	0.047	0.055	0.070	0.086	0.205
15	0.046	0.052	0.062	0.073	0.144
16	0.38	0.41	0.47	0.55	0.84
17	0.33	0.38	0.45	0.51	0.92
18	0.36	0.41	0.46	0.53	1.06
19	0.21	0.23	0.30	0.39	0.94
20	0.22	0.25	0.32	0.42	0.80
21	0.23	0.26	0.34	0.44	0.81
22	0.37	0.40	0.46	0.54	1.38
23	0.32	0.34	0.41	0.53	0.64
24	0.29	0.31	0.34	0.41	1.15
25	0.23	0.26	0.30	0.35	1.00
26	0.26	0.29	0.36	0.42	1.15
27	0.25	0.28	0.34	0.40	1.08
28	0.08	0.11	0.14	0.22	0.25

NOTES: Values in *italics* exceed the maximum feasible service-level bending moment for the specimen.

Table C-4: Midspan Deflections (from original sources) for Specific Levels of Midspan Bending Moment (Cont.)

Ref #	$\Delta_{test,6}$ (in.)	$\Delta_{test,7.5}$ (in.)	$\Delta_{test,10}$ (in.)	$\Delta_{test,12}$ (in.)	$\Delta_{test,max}$ (in.)
29	0.10	0.13	0.18	*0.23*	0.18
30	0.09	0.12	*0.22*	*0.38*	0.20
31	0.11	0.16	*0.33*	*0.54*	0.20
32	0.10	0.13	0.18	0.23	0.26
33	0.12	0.13	*0.21*	*0.33*	0.16
34	0.16	0.17	0.24	0.29	0.34
35	0.09	0.11	0.13	0.20	0.25
36	0.10	0.11	0.15	0.19	0.23
37	0.18	0.20	0.23	0.27	0.35
38	0.07	0.07	0.09	*0.14*	0.12
39	0.13	0.16	0.20	0.25	0.33
40	0.11	0.13	0.16	0.20	0.28
41	0.09	0.10	0.13	0.15	0.16
42	0.18	0.19	0.23	0.26	0.26
43	0.11	0.13	*0.16*	*0.19*	0.15
44	0.19	0.21	*0.25*	*0.28*	0.23
45	0.16	0.17	*0.21*	*0.23*	0.20
46	0.11	0.14	*0.20*	*0.30*	0.18
47	0.14	0.16	0.20	*0.23*	0.21
48	0.09	0.09	0.10	0.11	0.16
49	0.07	0.08	0.10	0.12	0.14
50	0.11	0.11	0.13	0.15	0.22
51	0.14	0.16	0.21	0.23	0.29
52	0.13	0.13	0.16	0.20	0.29
53	0.09	0.09	0.12	0.14	0.17
54	0.13	0.15	0.19	0.22	0.27
55	0.14	0.15	0.16	0.18	0.20
56	0.15	0.16	0.18	0.20	0.21

NOTES: Values in *italics* exceed the maximum feasible service-level bending moment for the specimen.

Table C-4: Midspan Deflections (from original sources) for Specific Levels of Midspan Bending Moment (Cont.)

Ref #	$\Delta_{test,6}$ (in.)	$\Delta_{test,7.5}$ (in.)	$\Delta_{test,10}$ (in.)	$\Delta_{test,12}$ (in.)	$\Delta_{test,max}$ (in.)
57	0.09	0.10	0.13	0.16	0.20
58	0.12	0.15	0.17	0.20	0.21
59	0.15	0.17	0.19	*0.22*	0.19
60	0.14	0.16	0.18	*0.21*	0.20
61	0.04	0.05	0.08	0.11	0.14
62	0.04	0.04	0.06	0.08	0.10
63	0.04	0.04	0.06	0.08	0.09
64	0.05	0.05	0.07	0.10	0.21
65	0.04	0.05	0.07	0.09	0.17
66	0.09	0.11	0.13	0.16	0.29
67	0.07	0.08	0.11	0.15	0.33
68	0.05	0.06	*0.13*	*0.22*	0.06
69	0.07	0.08	0.10	*0.12*	0.10
70	0.08	0.09	0.10	0.12	0.12
71	0.11	0.15	*0.22*	*0.35*	0.20
72	0.07	0.08	*0.17*	*0.24*	0.16
73	0.13	0.16	0.21	*0.23*	0.21
74	0.15	0.18	0.20	0.23	0.23
75	0.14	0.18	*0.25*	*0.28*	0.20
76	0.11	0.13	*0.19*	*0.24*	0.16
77	0.05	0.06	0.08	0.10	0.12
78	0.08	0.11	0.17	0.25	0.32
79	0.13	0.15	*0.19*	*0.37*	0.15
80	0.12	0.12	*0.24*	*0.39*	0.15
81	0.08	0.12	*0.20*	*0.28*	0.17
82	0.10	0.13	*0.19*	*0.24*	0.17
83	0.14	0.15	0.16	*0.21*	0.18
84	0.16	0.17	0.20	*0.23*	0.22

NOTES: Values in *italics* exceed the maximum feasible service-level bending moment for the specimen.

Table C-4: Midspan Deflections (from original sources) for Specific Levels of Midspan Bending Moment (Cont.)

Ref #	$\Delta_{test,6}$ (in.)	$\Delta_{test,7.5}$ (in.)	$\Delta_{test,10}$ (in.)	$\Delta_{test,12}$ (in.)	$\Delta_{test,max}$ (in.)
85	0.07	0.11	*0.19*	*0.27*	0.16
86	0.08	0.09	*0.18*	*0.27*	0.15
87	0.14	0.15	0.17	0.20	0.21
88	0.07	0.10	*0.17*	*0.25*	0.14
89	0.12	0.13	0.16	0.19	0.20
90	0.14	0.16	*0.21*	*0.24*	0.20
91	0.16	0.17	0.21	0.25	0.29
92	0.16	0.16	0.20	*0.24*	0.23
93	0.09	0.10	*0.19*	*0.26*	0.15
94	0.13	0.14	0.18	0.23	0.24
95	0.15	0.18	0.24	0.26	0.29
96	0.15	0.17	*0.24*	*0.30*	0.18
97	0.12	0.13	0.18	0.22	0.24
98	0.09	0.10	0.12	0.15	0.15
99	0.12	0.14	0.16	0.20	0.20
100	0.10	0.12	0.15	0.18	0.19
101	0.06	0.07	0.08	*0.14*	0.09
102	0.09	0.09	0.11	0.14	0.24
103	0.12	0.13	0.16	0.18	0.23
104	0.06	0.07	0.12	*0.21*	0.15
105	0.09	0.10	0.11	0.17	0.30
106	0.13	0.14	0.17	0.19	0.25

NOTES: Values in *italics* exceed the maximum feasible service-level bending moment for the specimen.